Reduction-Based Control of Three-Dimensional Bipedal Walking Robots

Robert D. Gregg and Mark W. Spong

Abstract

This paper develops the concept of reduction-based control, which is founded on a controlled form of geometric reduction known as *functional Routhian reduction*. We prove a geometric property of general serial-chain robots termed *recursive cyclicity*, identifying the inherent robot symmetries that we exploit with the *Subrobot Theorem*. This shows that any serial-chain robot can be decomposed for arbitrarily lower-dimensional analysis and control. We apply this method to construct stable directional 3-D walking gaits for a 4-DOF hipped bipedal robot. The controlled reduction decouples the biped's sagittal-plane motion from the yaw and lean modes, and on the sagittal subsystem we use passivity-based control to produce known planar limit cycles on flat ground. The unstable yaw and lean modes are separately controlled to 2-periodic orbits through their shaped momenta. We numerically verify the existence of stable 2-periodic straight-walking limit cycles and demonstrate turning capabilities for the controlled biped.

I. Introduction

The implications of understanding bipedal locomotion are great due to its human application. The potential for improving prosthetic limbs, navigating uneven terrestrial surfaces, and creating efficient locomotive mechanisms are among the many incentives that drive research in this field of robotics. The humanoid form of locomotion known as dynamic bipedal walking is based on "controlled falling," where each leg's step cycle involves a fall towards the ground until foot impact transfers this falling motion to the other leg (enabling a hybrid sense of stability for the walking gait). This is quite different from the "quasi-static" locomotion of the popular Honda Asimo and Sony Qrio robots. These sophisticated bipeds maintain a static sense of stability during the entirety of each step cycle, resulting in somewhat unnatural and inefficient shuffling motion (Kuo, 2007).

The first significant studies in dynamic bipedal walking concerned simple models constrained to the sagittal plane (2-D space), such as the uncontrolled two-link "compass-gait" biped of Fig. 1, to roughly approximate human dynamic motion. McGeer discovered the existence of stable "passive" limit cycles down shallow slopes for the compass-gait biped in (McGeer, 1990), and passive dynamic walking was further studied in (Goswami et al., 1996). Grizzle et al. proved that stable limit cycles could be generated for underactuated planar walkers using a control

R. D. Gregg is with the Department of Electrical and Computer Engineering, University of Illinois at Urbana-Champaign, Urbana, IL 61801 rgregg@ieee.org

M. W. Spong is with the Department of Electrical Engineering, University of Texas at Dallas, Richardson, TX 75080 mspong@utdallas.edu

This research was supported by NSF Grant CMS-0510119. Preliminary results of this paper were presented in (Gregg and Spong, 2008).

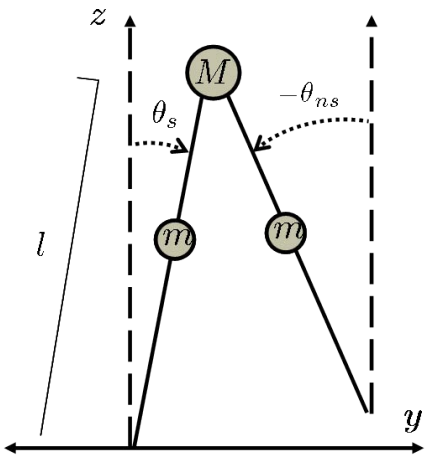

Fig. 1. The sagittal-plane "compass-gait" bipedal robot.

method known as hybrid zero dynamics (Westervelt et al., 2003), (Morris and Grizzle, 2006), in which output linearization is employed to zero hybrid-invariant output functions (i.e., virtual constraints) describing the walking gait. These walking gaits were demonstrated on the planar RABBIT bipedal robot at the Laboratoire Automatique de Grenoble in France (Chevallereau et al., 2003).

Although these concepts have been quite successful with regard to planar walking mechanisms, there has been scattered success in extending these ideas to the three-dimensional (3-D) case, where robot dynamics become quite complex with several highly-coupled degrees-of-freedom (DOF). Tedrake et al. confront dynamic complexity and terrain uncertainty for a planar compass-gait biped by discretizing the state space and dynamics, so as to analyze the stochastic "metastability" of the resulting controlled Markov chain (Byl and Tedrake, 2008). However, the mesh state space expands exponentially with the robot's dimensionality, bringing into question this method's practicality for high-DOF bipeds in three dimensions. On the other hand, (Tedrake et al., 2004) apply stochastic learning to a simple experimental biped in three dimensions, assuming the frontal and sagittal planes-of-motion are decoupled and using large feet to help compensate for swaying.

Passive dynamic walking was extended to a spatially 3-D biped (pitch and lean modeled without yaw) in (Kuo, 1999), requiring direct control over the leg splay angle and an assumption that the continuous dynamics are invariant under this actuation. Collins built an impressive mechanism that demonstrated 3-D passive dynamic walking (Collins et al., 2001), after being carefully tuned to walk straight down a particular fixed slope from a specific initial configuration. Spong and Bullo introduced passivity-based control and controlled symmetries in (Spong, 1999), (Spong, 2004), (Spong and Bullo, 2005), showing that 3-D passive limit cycles on shallow slopes could be mapped to 3-D "pseudo-passive" limit cycles on arbitrary slopes with expanded basins of attraction (and with trajectory time-scaling in (Spong et al., 2007)). Since this requires the existence of stable passive limit cycles, which is usually not the case for complex 3-D bipedal walkers, the primary application of this method has been limited to sagittal-plane walking (such as the compass-gait biped).

In the recent paper (Chevallereau et al., 2008), the method of hybrid zero dynamics is extended to spatially 3-D bipedal walkers by employing various optimality criteria. In related work (Fukuda et al., 2006), spatial 3-D walking is achieved by assuming that the sagittal and lateral dynamics are decoupled and can be separately controlled using virtual constraints that define appropriate zero dynamics. However, we argue that these planes of motion are naturally strongly coupled, especially in the case of a hipped walker with significant swaying motion, requiring a more sophisticated method of decomposing a biped's walking motion.

Extensive work has demonstrated that passivity-based methods can build natural and efficient dynamic walking gaits for planar robots, based on gravity-powered passive dynamics, but most 3-D bipeds cannot stably exploit passive dynamics. Studying this problem, Ames et al. observed that a 3-D biped's gait dynamics are dominated by its sagittal plane-of-motion (Ames et al., 2006), (Ames and Gregg, 2007), (Ames et al., 2007). This suggested that geometric reduction might be used to isolate the sagittal 2-D subsystem, which is better understood, and from this build a pseudo-passive 3-D walking gait. The reduction could "decouple" the walker's sagittal-plane motion from the lean mode of the frontal (or lateral) plane and the yaw mode of the axial (or transverse) plane, and known planar walking cycles could be generated on this sagittal subsystem using passivity-based control methods.

In particular, geometric reduction is an analytical method of decomposing a physical system, often characterized by a Lagrangian function, with symmetries that are invariant under the action of a Lie group on the configuration space. A few such forms of reduction are discussed in (Marsden and Ratiu, 2002), such as Lie-Poisson, Euler-Poincaré, and Routh. In the classical form of *Routhian reduction*, a Lagrangian L has configuration space $\mathcal{Q} = \mathbb{G} \times S$ (usually an n-torus), where $\mathbb{G} = \mathbb{G}_1 \times \ldots \times \mathbb{G}_k$ is a *symmetry group* and $S \cong \mathcal{Q} \backslash \mathbb{G}$ is the *shape space*. Symmetries of L are characterized by *cyclic* variables $q_i \in \mathbb{G}_i$, which are variables that do not explicitly appear in L:

$$\frac{\partial L}{\partial q_i} = 0, \quad i \in \{1, k\}. \tag{1}$$

By dividing out the symmetry group $\mathbb{G}$, the full-order phase space $T\mathcal{Q}$ projects onto the reduced-order phase space TS. Moreover, Equation (1) implies that each cyclic coordinate's generalized momentum is constant. When system dynamics evolve on level-sets of these conserved momentum quantities, the symmetries allow us to directly relate the behavior of the full-order system and the reduced system. In other words, solutions on the reduced system uniquely imply solutions on the full-order system and vice versa. A similar notion of reduction is elegantly applied to geometric motion planning of underactuated mechanical systems in (Shammas et al., 2007a), (Shammas et al., 2007b), using the reduced system to produce motion along unactuated coordinates corresponding to the symmetry group.

In our context of dynamics and control, reduced system stability corresponds to stability in phase space $TS \cong T\mathcal{Q}$ modulo $T\mathbb{G}$. This says nothing about the stability of the divided coordinates of $T\mathbb{G}$ (which in the case of bipedal walking will be the unstable lean and yaw modes). Motivated by symmetry-breaking stabilization techniques applied to underwater vehicles (Leonard, 1997) and wave equations (Mehta et al., 2007), Ames et al. use energy-shaping control to break the symmetry of group $\mathbb{G}$ in order to stabilize orbits of $T\mathbb{G}$. However, symmetry-breaking is imposed in a specific manner so as to preserve the projection map, so that the group $\mathbb{G}$ of "almost-cyclic" variables can still be divided. This controlled variant of Routhian reduction, *functional Routhian reduction*, shapes the system

energy to dynamically alter the momentum of the divided coordinate, whereby the divided space is controlled. This is demonstrated on spatial 3-DOF bipeds, for which controlled reduction of the lean dynamics results in fixed-heading walking gaits. However, modeling yaw in a 4-DOF biped does not result in a single symmetry group for both the yaw and lean coordinates (lean is no longer cyclic), so this method could not be applied to a completely 3-D biped to incorporate direction/heading.

In this paper, we wish to allow arbitrary dimensionality reduction, in order to reduce and control both the yaw and lean modes from a completely 3-D biped. Therefore, in Section II we present a generalized multistage form of the controlled reduction method, as proposed in (Gregg and Spong, 2008). We show in Section III that robots have extensive "nested" symmetries that can be exploited for multistage reduction by proving the geometric property of serial-chain robot inertia matrices termed *recursive cyclicity*. This property leads to our proof of the *Subrobot Theorem*, which shows that any serial-chain robot can be decomposed for lower-dimensional analysis and controlled as a simpler "subrobot." Although the presented theory is based on symmetries inherent in serial chains, this can be generalized to branched chains as done in (Gregg and Spong, 2009b).

In the context of 3-D bipedal walking, these theoretical results simplify the search for full-order limit cycles (since we build from sagittal-plane stability) and expand the class of robots that can achieve pseudo-passive dynamic walking in three dimensions. We begin the demonstration of this principle by describing our model of application, a 4-DOF bipedal walker with a hip and splayed legs, in Section IV. We then design a reduction-based control law in Section V to impose a 2-stage controlled reduction to the robot's sagittal-plane subsystem, on which we use passivity-based control to build robust limit cycles on flat ground. As a result of the controlled reduction, lean is forced to vertical and yaw is forced to the desired heading angle between steps. We show in Section VI that this control method results in stable directional limit cycles on flat ground, which are 2-periodic due to the side-to-side lateral swaying and axial turning motions induced by the robot's hip. This nicely resembles human-like walking. We are unaware of any other results in dynamic walking, aside from our introductory work, that allow for directional control – the closest would be the quasi-static Asimo biped and others like it.

II. Controlled Reduction

We discuss controlled reduction by first presenting the k-stage variant of functional Routhian reduction for an n-DOF robot, where $1 \leq k < n$, based on the construction from the single-stage case of (Ames, 2006), (Ames et al., 2007). This provides for recursive reduction of robot dynamics, derived from a special Lagrangian function, to a lower-dimensional subsystem while separately controlling the divided variables. We then identify the inherent robot symmetries that allow this method to be applied to any serial chain by the Subrobot Theorem. In order to lay the necessary Lagrangian framework, we begin by describing a robot's typical Lagrangian dynamics.

A. Lagrangian Dynamics

A mechanical system with configuration space $\mathcal{Q}$ is described by elements $(q, \dot{q})$ of the tangent bundle $T\mathcal{Q}$ (space of configuration and velocities) and the Lagrangian function $L : T\mathcal{Q} \to \mathbb{R}$, given in coordinates by

$$L(q, \dot{q}) = K(q, \dot{q}) - V(q) = \frac{1}{2}\dot{q}^T M(q)\dot{q} - V(q),$$

where $K(q, \dot{q})$ is the kinetic energy, $V(q)$ is the potential energy, and $M(q)$ is the $n \times n$ symmetric, positive-definite mass/inertia matrix. Since the Lagrangian satisfies the n-dimensional controlled Euler-Lagrange (E-L) equations,

$$\frac{d}{dt}\frac{\partial L}{\partial \dot{q}} - \frac{\partial L}{\partial q} = Bu,$$

the dynamical equations of motion for the controlled robot are given with the special structure

$$M(q)\ddot{q} + C(q, \dot{q})\dot{q} + N(q) = Bu,$$

where $n \times n$-matrix $C(q, \dot{q})$ contains the Coriolis and centrifugal terms, $N(q) = \frac{\partial}{\partial q}V(q)$ is the vector of potential (e.g., gravitational) torques, $n \times n$-matrix B is assumed invertible for full actuation, and control input u is an n-dimensional vector of joint actuator torques.

These equations yield the dynamical control system (f, g):

$$\begin{pmatrix} \dot{q} \\ \ddot{q} \end{pmatrix} = f(q, \dot{q}) + g(q)u \tag{2}$$

with vector field f and matrix g of control vector fields:

$$f(q, \dot{q}) = \begin{pmatrix} \dot{q} \\ M(q)^{-1}\left(-C(q, \dot{q})\dot{q} - N(q)\right) \end{pmatrix}, \quad g(q) = \begin{pmatrix} 0_{n\times n} \\ M(q)^{-1}B \end{pmatrix}.$$

If this Lagrangian has cyclic variables, as in (1), that are free from external forces (e.g., no actuation), we can decompose the dynamics with Routh reduction. However, in order to control these variables, we must describe a special class of Lagrangians that instead have "almost-cyclic" variables.

B. k-Almost-Cyclic Lagrangians

We start with a general n-dimensional configuration space $\mathcal{Q} = \mathbb{T}^k \times S$, where shape space $S \cong \mathcal{Q}\backslash\mathbb{T}^k$ is constructed by $n - k$ copies of $\mathbb{R}$ and circle $\mathbb{S}^1$, and $\mathbb{T}^k = \mathbb{S}^1 \times \ldots \times \mathbb{S}^1$ is the group of "almost-cyclic" variables to be divided one copy of $\mathbb{S}^1$ at a time. We denote a configuration $q \in \mathcal{Q}$ by $q = (q_1, \ldots, q_n)^T = ({q_1^i}^T, {q_{i+1}^n}^T)^T$ for $1 \leq i \leq n$, with i-dimensional vector q_1^i containing coordinates $q_1, \ldots, q_i$ and $(n - i)$-dimensional vector q_{i+1}^n containing coordinates $q_{i+1}, \ldots, q_n$ (clearly if $i = n$ then $q_{n+1}^n = \emptyset$). In particular, for $i = k$ we have the vector of almost-cyclic variables $q_1^k \in \mathbb{T}^k$ and the vector of shape space variables $q_{k+1}^n \in S$. To begin, let inertia matrix M be defined from a class of *recursively cyclic* matrices, giving us the symmetries we need for reduction.

Definition 1: An $n \times n$-matrix M is *recursively cyclic* if each lower-right $(n-i+1) \times (n-i+1)$ submatrix is cyclic in $q_1, \ldots, q_i$ for $1 \leq i \leq n$, i.e., it has the form

$$
\begin{aligned}
M(q_2^n) &= \begin{pmatrix} m_{q_1}(q_2^n) & M_{q_1,q_2^n}(q_2^n) \\ M^T_{q_1,q_2^n}(q_2^n) & M_{q_2^n}(q_3^n) \end{pmatrix} \\
&= \begin{pmatrix} m_{q_1}(q_2^n) & \multicolumn{1}{c}{\text{—}} & M_{q_1,q_2^n}(q_2^n) & \multicolumn{1}{c}{\text{———}} \\ | & \ddots & & \vdots \\ M^T_{q_1,q_2^n}(q_2^n) & & m_{q_{i-1}}(q_i^n) & M_{q_{i-1},q_i^n}(q_i^n) \\ | & \cdots & M^T_{q_{i-1},q_i^n}(q_i^n) & M_{q_i^n}(q_{i+1}^n) \end{pmatrix}
\end{aligned} \tag{3}
$$

with the base case $i = n$ where $M_{q_n^n}(q_{n+1}^n) = m_{q_n} \in \mathbb{R}$ is a scalar constant.

Remark 1: In our context, for $1 \leq j \leq n$, each $m_{q_j}(q_{j+1}^n)$ is the scalar positive-definite self-induced inertia term of coordinate q_j, $M_{q_j,q_{j+1}^n}(q_{j+1}^n) \in \mathbb{R}^{j-1}$ is the row vector of off-diagonal inertial coupling terms between q_j and coordinates q_{j+1}^n, and $M_{q_j^n}(q_{j+1}^n) \in \mathbb{R}^{(n-j+1)\times(n-j+1)}$ is the symmetric positive-definite inertia submatrix of coordinates q_j^n.

A special class of shaped Lagrangians termed *almost-cyclic Lagrangians* is defined in (Ames et al., 2007), allowing one stage of controlled reduction to a subsystem characterized by a *functional Routhian* – the Lagrangian function of the lower-dimensional system. In order to control k divided variables, each stage of reduction must project from an almost-cyclic Lagrangian (ACL) to a functional Routhian that is also almost-cyclic for the next stage of reduction (except the final stage to be discussed later). In other words, each subrobot's parent ACL must contain a nested lower-dimensional ACL (except again for the base case). Therefore, we are interested in a generalized form of the almost-cyclic Lagrangians presented in (Ames et al., 2007).

Definition 2: A Lagrangian $L_{\lambda_1^k} : T\mathbb{T}^k \times TS \to \mathbb{R}$ is *k-almost-cyclic* if, in coordinates, it has the form

$$
\begin{aligned}
L_{\lambda_1^k}(q,\dot{q}) &:= K_{\lambda_1^k}(q,\dot{q}) + Q^T_{\lambda_1^k}(q)\dot{q} - V_{\lambda_1^k}(q) && \text{(4a)} \\
&:= L_{\lambda_2^k}(q_2^n,\dot{q}_2^n) + \frac{1}{2}m_{q_1}(q_2^n)(\dot{q}_1)^2 + \dot{q}_1 M_{q_1,q_2^n}(q_2^n)\dot{q}_2^n && \text{(4b)} \\
&\quad + \frac{1}{2}\dot{q}_2^{n\,T}\frac{M^T_{q_1,q_2^n}(q_2^n)M_{q_1,q_2^n}(q_2^n)}{m_{q_1}(q_2^n)}\dot{q}_2^n - \frac{\lambda_1(q_1)}{m_{q_1}(q_2^n)}M_{q_1,q_2^n}(q_2^n)\dot{q}_2^n + \frac{1}{2}\frac{\lambda_1(q_1)^2}{m_{q_1}(q_2^n)},
\end{aligned}
$$

where the kinetic energy, inertia matrix, gyroscopic terms, and potential energy are respectively defined by

$$
\begin{aligned}
K_{\lambda_1^k}(q,\dot{q}) &= \frac{1}{2}\dot{q}^T M_{\lambda_1^k}(q_2^n)\dot{q} && (5) \\
M_{\lambda_1^k}(q_2^n) &= M(q_2^n) + \sum_{i=1}^{k}\begin{pmatrix} 0_{i\times i} & 0_{i\times(n-i)} \\ 0_{(n-i)\times i} & \frac{M^T_{q_i,q_{i+1}^n}(q_{i+1}^n)M_{q_i,q_{i+1}^n}(q_{i+1}^n)}{m_{q_i}(q_{i+1}^n)} \end{pmatrix} && (6) \\
Q_{\lambda_1^k}(q) &= \sum_{i=1}^{k}\begin{pmatrix} 0 & -\frac{\lambda_i(q_i)}{m_{q_i}(q_{i+1}^n)}M_{q_i,q_{i+1}^n}(q_{i+1}^n) \end{pmatrix}^T && (7) \\
V_{\lambda_1^k}(q) &= V_{\text{fct}}(q_{k+1}^n) - \frac{1}{2}\sum_{i=1}^{k}\frac{\lambda_i(q_i)^2}{m_{q_i}(q_{i+1}^n)}, && (8)
\end{aligned}
$$

for some functions $\lambda_i : \mathbb{S}^1 \to \mathbb{R}$, $i \in \{1, k\}$, and target potential energy V_{fct} after k stages of functional reduction.

Remark 2: The closed-form definition of (4a) explicitly shows all the shaping terms necessary for k stages of controlled reduction, whereas the last three terms in the recursive definition of (4b) impose the controlled reduction to the first stage's target $(k-1)$-almost-cyclic Lagrangian, $L_{\lambda_2^k}$, to be defined later.

Given a k-almost-cyclic Lagrangian (k-ACL) $L_{\lambda_1^k}$, the n-dimensional fully-actuated E-L equations yield

$$M_{\lambda_1^k}(q_2^n)\ddot{q} + C_{\lambda_1^k}(q,\dot{q})\dot{q} + N_{\lambda_1^k}(q) = Bv, \tag{9}$$

where $C_{\lambda_1^k}$ is the k-almost-cyclic Coriolis-gyroscopic matrix (see Appendix A), $N_{\lambda_1^k} = \frac{\partial}{\partial q} V_{\lambda_1^k}$ is the vector of k-almost-cyclic potential torques, B is an invertible matrix, and v is the n-dimensional control input vector. Then, we have the control system on $T\mathcal{Q}$ associated with $L_{\lambda_1^k}$, $(f_{\lambda_1^k}, g_{\lambda_1^k})$, defined as usual:

$$\begin{pmatrix} \dot{q} \\ \ddot{q} \end{pmatrix} = f_{\lambda_1^k}(q,\dot{q}) + g_{\lambda_1^k}(q)v. \tag{10}$$

Letting v_{k+1}^n be the subsystem control law on TS, we incorporate this into the full-order k-ACL system by defining the new control system $(\hat{f}_{\lambda_1^k}, \hat{g}_{\lambda_1^k})$ with input v_1^k:

$$\begin{aligned} \hat{f}_{\lambda_1^k}(q,\dot{q}) &:= f_{\lambda_1^k}(q,\dot{q}) + g_{\lambda_1^k}(q) \begin{pmatrix} 0_{k\times(n-k)} \\ I_{(n-k)\times(n-k)} \end{pmatrix} v_{k+1}^n \\ \hat{g}_{\lambda_1^k}(q) &:= g_{\lambda_1^k}(q) \begin{pmatrix} I_{k\times k} \\ 0_{(n-k)\times k} \end{pmatrix}, \end{aligned} \tag{11}$$

where v_1^k is the k-dimensional vector containing the first k elements of input v, and v_{k+1}^n is the $(n-k)$-dimensional vector containing the remaining elements $k+1, \ldots, n$. Here, vector field $\hat{f}_{\lambda_1^k}$ corresponds to the v_{k+1}^n-controlled E-L equations (absent of control v_1^k), which will be relevant to the reduction theorem to be discussed. Moreover, we prove in Appendix A that k-almost-cyclic systems preserve the inertia matrix, skew-symmetry, and passivity properties of robotic systems.

C. Reduced Subsystems

Starting with the full-order k-ACL system described above, each stage of reduction projects onto a lower-dimensional system characterized by a Routhian function, while conserving a momentum quantity corresponding to the divided degree-of-freedom. Although these coordinates do not explicitly appear in the reduced-order systems, they can be uniquely reconstructed by the *functional momentum maps* $J_j : T(\mathcal{Q}\backslash\mathbb{T}^{j-1}) \to \mathbb{R}$, $j \in \{1, k\}$:

$$\begin{aligned} J_j(q_j^n, \dot{q}_j^n) &= \frac{\partial}{\partial \dot{q}_j} L_{\lambda_j^k}(q_j^n, \dot{q}_j^n) \\ &= M_{q_j, q_{j+1}^n}(q_{j+1}^n)\dot{q}_{j+1}^n + m_{q_j}(q_{j+1}^n)\dot{q}_j \\ &= \lambda_j(q_j). \end{aligned} \tag{12}$$

Here, $L_{\lambda_j^k}$ is the k-ACL for $j = 1$ or the stage-$(j-1)$ functional Routhian, to be defined next, for $j \in \{2, k\}$. Since we wish to control the divided variables, the energy shaping terms in $L_{\lambda_1^k}$ break each conservative map

J_j (traditionally constant under (1) and the uncontrolled E-L equations) and force it equal to a desirable function $\lambda_j(q_j)$. Hence, we control the momenta of the divided coordinates.

In this framework of multistage functional Routh reduction, k stages of reduction yield k functional Routhians. For $j \in \{2, k\}$, the functional Routhian corresponding to the $(j-1)^{\text{st}}$ stage of reduction is a $(k-j+1)$-ACL[1] on the tangent bundle of reduced configuration space $\mathcal{Q}\backslash\mathbb{T}^{j-1}$. In other words, the first $k-1$ functional Routhians are generalized almost-cyclic Lagrangians that allow for further stages of controlled reduction. Therefore, we have the following definition for a generalized functional Routhian.

Definition 3: Given k-ACL $L_{\lambda_1^k}$, the *stage-$(j-1)$ functional Routhian* $L_{\lambda_j^k} : T(\mathcal{Q}\backslash\mathbb{T}^{j-1}) \to \mathbb{R}$ is obtained through a partial Legendre transformation in variable q_{j-1}:

$$
\begin{aligned}
L_{\lambda_j^k}(q_j^n, \dot{q}_j^n) &:= \left[L_{\lambda_{j-1}^k}(q_{j-1}^n, \dot{q}_{j-1}^n) - \lambda_{j-1}(q_{j-1})\dot{q}_{j-1}\right]\Big|_{J_{j-1}(q_{j-1}^n, \dot{q}_{j-1}^n)=\lambda_{j-1}(q_{j-1})} \\
&= K_{\lambda_j^k}(q_j^n, \dot{q}_j^n) + Q_{\lambda_j^k}^T(q_j^n)\dot{q}_{j+1}^n - V_{\lambda_j^k}(q_j^n) \qquad (13a) \\
&= L_{\lambda_{j+1}^k}(q_{j+1}^n, \dot{q}_{j+1}^n) + \frac{1}{2}m_{q_j}(q_{j+1}^n)(\dot{q}_j)^2 + \dot{q}_j M_{q_j, q_{j+1}^n}(q_{j+1}^n)\dot{q}_{j+1}^n \qquad (13b) \\
&\quad + \frac{1}{2}{\dot{q}_{j+1}^n}^T \frac{M_{q_j, q_{j+1}^n}^T(q_{j+1}^n) M_{q_j, q_{j+1}^n}(q_{j+1}^n)}{m_{q_j}(q_{j+1}^n)} \dot{q}_{j+1}^n \\
&\quad - \frac{\lambda_j(q_j)}{m_{q_j}(q_{j+1}^n)} M_{q_j, q_{j+1}^n}(q_{j+1}^n)\dot{q}_{j+1}^n + \frac{1}{2}\frac{\lambda_j(q_j)^2}{m_{q_j}(q_{j+1}^n)},
\end{aligned}
$$

where the kinetic energy, inertia matrix, gyroscopic terms, and potential energy are respectively defined by

$$
\begin{aligned}
K_{\lambda_j^k}(q_j^n, \dot{q}_j^n) &= \frac{1}{2}{\dot{q}_j^n}^T M_{\lambda_j^k}(q_{j+1}^n)\dot{q}_j^n \\
M_{\lambda_j^k}(q_{j+1}^n) &= M_{q_j^n}(q_{j+1}^n) + \sum_{i=j}^{k} \begin{pmatrix} 0_{i\times i} & 0_{i\times(n-i)} \\ 0_{(n-i)\times i} & \frac{M_{q_i, q_{i+1}^n}^T(q_{i+1}^n) M_{q_i, q_{i+1}^n}(q_{i+1}^n)}{m_{q_i}(q_{i+1}^n)} \end{pmatrix} \\
Q_{\lambda_j^k}(q_j^n) &= \sum_{i=j}^{k} \begin{pmatrix} 0 & -\frac{\lambda_i(q_i)}{m_{q_i}(q_{i+1}^n)} M_{q_i, q_{i+1}^n}(q_{i+1}^n) \end{pmatrix}^T \\
V_{\lambda_j^k}(q_j^n) &= V_{\text{fct}}(q_{k+1}^n) - \frac{1}{2}\sum_{i=j}^{k} \frac{\lambda_i(q_i)^2}{m_{q_i}(q_{i+1}^n)},
\end{aligned}
$$

for $j \in \{2, k\}$.

The final stage of reduction, stage-k, is a functional Routhian $L_{\text{fct}} = L_{\lambda_{k+1}^k}$ of the form presented for single-stage controlled reduction in (Ames et al., 2007). This is obtained from the 1-almost-cyclic Routhian $L_{\lambda_k^k}$ of stage-$(k-1)$ through a partial Legendre transformation in the variable q_k with the constraint $J_k(q_k^n, \dot{q}_k^n) = \lambda_k(q_k)$. It follows that the corresponding stage-k functional Routhian $L_{\text{fct}} : TS \cong T(\mathcal{Q}\backslash\mathbb{T}^k) \to \mathbb{R}$, which is the Lagrangian of the

[1]Note that the stage-$(j-1)$ functional Routhian is also $(j-1)$-cyclic within the original configuration space $\mathcal{Q}$, but we are working in the reduced configuration space $\mathcal{Q}\backslash\mathbb{T}^{j-1}$ and are concerned with almost-cyclic characteristics for further controlled reduction.

k-reduced subsystem, is given in coordinates by

$$\begin{aligned} L_{\text{fct}}(q^n_{k+1}, \dot{q}^n_{k+1}) &:= \left[L_{\lambda^k_k}(q^n_k, \dot{q}^n_k) - \lambda_k(q_k)\dot{q}_k\right]\Big|_{J_k(q^n_k,\dot{q}^n_k)=\lambda_k(q_k)} \\ &= \frac{1}{2}\dot{q}^{n^T}_{k+1} M_{q^n_{k+1}}(q^n_{k+1})\dot{q}^n_{k+1} - V_{\text{fct}}(q^n_{k+1}). \end{aligned} \tag{14}$$

Therefore, the $(n-k)$-dimensional controlled E-L equations of L_{fct} yield

$$M_{q^n_{k+1}}(q^n_{k+1})\ddot{q}^n_{k+1} + C_{q^n_{k+1}}(q^n_{k+1}, \dot{q}^n_{k+1})\dot{q}^n_{k+1} + N_{\text{fct}}(q^n_{k+1}) = B_{q^n_{k+1}} v^n_{k+1},$$

where $C_{q^n_{k+1}}$ and N_{fct} are defined as usual, and $B_{q^n_{k+1}}$ is the invertible $(n-k)\times(n-k)$ lower-right submatrix of B corresponding to coordinates q^n_{k+1}. Then, we have the control system on TS associated with L_{fct}, $(f_{\text{fct}}, g_{\text{fct}})$:

$$\begin{pmatrix} \dot{q}^n_{k+1} \\ \ddot{q}^n_{k+1} \end{pmatrix} = f_{\text{fct}}(q^n_{k+1}, \dot{q}^n_{k+1}) + g_{\text{fct}}(q^n_{k+1}) v^n_{k+1}. \tag{15}$$

From this, we can define the vector field corresponding to the k-reduced, controlled E-L equations:

$$\hat{f}_{\text{fct}}(q^n_{k+1}, \dot{q}^n_{k+1}) := f_{\text{fct}}(q^n_{k+1}, \dot{q}^n_{k+1}) + g_{\text{fct}}(q^n_{k+1}) v^n_{k+1}. \tag{16}$$

D. Controlled Reduction Theorem

Now that we have defined the full-order and reduced systems, we can introduce the Theorem relating their behavior. When control v^k_1 is absent and the functional momentum quantities are conserved according to (12), there exists a map between solutions of full-order vector field $\hat{f}_{\lambda^k_1}$ and reduced-order vector field $\hat{f}_{\text{fct}}$. The following is a direct generalization of the single-stage result presented in (Ames et al., 2007).

Theorem 1: Let $L_{\lambda^k_1}$ be a k-almost-cyclic Lagrangian with corresponding stage-k functional Routhian L_{fct}. Then $(q^k_1(t), q^n_{k+1}(t), \dot{q}^k_1(t), \dot{q}^n_{k+1}(t))$ is a solution to the v^n_{k+1}-controlled vector field $\hat{f}_{\lambda^k_1}$ on $[t_0, t_f]$ with

$$\dot{q}_j(t_0) = \frac{1}{m_{q_j}(q^n_{j+1}(t_0))}\left(\lambda_j(q_j(t_0)) - M_{q_j, q^n_{j+1}}(q^n_{j+1}(t_0))\dot{q}^n_{j+1}(t_0)\right), \tag{17}$$

for all $j \in \{1, k\}$, if and only if $(q^n_{k+1}(t), \dot{q}^n_{k+1}(t))$ is a solution to the controlled vector field $\hat{f}_{\text{fct}}$ and $(q_j(t), \dot{q}_j(t))$ satisfies

$$\dot{q}_j(t) = \frac{1}{m_{q_j}(q^n_{j+1}(t))}\left(\lambda_j(q_j(t)) - M_{q_j, q^n_{j+1}}(q^n_{j+1}(t))\dot{q}^n_{j+1}(t)\right), \tag{18}$$

for all $j \in \{1, k\}$.

The proof of this theorem, which involves lengthy calculations, can be found in Appendix B. We want to apply this form of controlled reduction to general robots, but we certainly cannot expect robots to naturally be k-almost-cyclic. Therefore, we must show that any serial-chain robot has a recursively-cyclic inertia matrix and that a feedback control law exists that yields a shaped k-ACL to allow for k stages of controlled reduction. In other words, we will prove the existence of a class of control laws termed "reduction-based" controllers.

III. The Subrobot Theorem

We now lay the framework for the Subrobot Theorem, which shows that multistage controlled reduction can decompose any serial-chain robot for lower-dimensional analysis and control. This first brings us to prove the geometric property of recursive cyclicity of inertia matrices, as proposed in (Gregg and Spong, 2008).

Lemma 1: The kinetic energy $K(q,\dot{q}) = \frac{1}{2}\dot{q}^T M(q)\dot{q}$ of any n-DOF serial kinematic chain is cyclic in coordinate q_1 corresponding to the first DOF, i.e., $\frac{\partial}{\partial q_1}K(q,\dot{q}) = 0$. Equivalently, inertia matrix $M(q)$ is cyclic in q_1.

Proof: It is shown in (Spong and Bullo, 2002) that the kinetic energy of an n-DOF robot is invariant under rotations of the world coordinate frame. This property follows from the fact that the mass/inertia of a single link is constant, and all other links are relative to the first link. Therefore, the kinetic energy, being the sum of link kinetic energies as detailed in (Spong et al., 2006), is invariant under the orientation of the first link (relative to the world frame). Since the first degree-of-freedom is always referenced to the world frame, it follows that $\frac{\partial}{\partial q_1}K(q,\dot{q}) = 0$ and thus q_1 is a cyclic coordinate with respect to kinetic energy. ■

Lemma 2: The $n\times n$ inertia matrix M of any n-DOF serial kinematic chain contains a lower-right $(n-1)\times(n-1)$ submatrix $M_{q_2^n}$, which is the inertia matrix of the $(n-1)$-DOF subrobot with coordinates q_2^n corresponding to the original robot with its first DOF fixed.

Proof: Fix $q_1 = c$, $\dot{q}_1 = 0$, where c is constant. The top-most row and left-most column of M are zeroed in the constrained kinetic energy

$$K(q,\dot{q})|_{q_1=c,\dot{q_1}=0} \quad = \quad \frac{1}{2}\dot{q}^T M(q)\dot{q}\Big|_{q_1=c,\dot{q_1}=0}.$$

Since M is cyclic by Lemma 1, the lower-right $(n-1)\times(n-1)$ submatrix $M_{q_2^n}$ is invariant under this constraint. Then, this constrained kinetic energy is equal to the $(n-1)$-DOF subrobot's kinetic energy:

$$K(q,\dot{q})|_{q_1=c,\dot{q_1}=0} \quad = \quad \frac{1}{2}{\dot{q}_2^n}^T M_{q_2^n}(q_2^n)\dot{q}_2^n \quad = \quad K_2(q_2^n,\dot{q}_2^n).$$

Equivalently, submatrix $M_{q_2^n}$ is the inertia matrix of this subrobot. ■

Theorem 2: For some choice of generalized coordinates, the inertia matrix of any serial kinematic chain is recursively cyclic as in Definition 1.

Proof: We begin this proof by induction by examining the cyclicity of the base case. The 1-DOF subrobot corresponding to the lower-rightmost (scalar) submatrix of an n-DOF inertia matrix is trivially cyclic within the 1-DOF subconfiguration, since the mass/inertia of a single link is constant (as argued in the proof of Lemma 1).

As for the general case, consider the m-DOF subrobot of an n-DOF serial chain, where $1 < m \leq n$. As described earlier, this m-DOF subrobot is simply the n-DOF robot with the first $n-m$ coordinates fixed (note that these fixed coordinates do not affect the m-DOF submatrix as argued in the proof of Lemma 2). This subrobot's inertia matrix $M_{q^n_{n-m+1}}$, which is cyclic in q_{n-m+1} by Lemma 1 (within the m-DOF subconfiguration), contains an $(m-1)$-DOF subrobot's inertia matrix $M_{q^n_{n-m+2}}$ by Lemma 2. Fixing cyclic coordinate q_{n-m+1}, submatrix $M_{q^n_{n-m+2}}$ is then cyclic with respect to the next coordinate q_{n-m+2} by Lemma 1 (now within the $(m-1)$-DOF subconfiguration) and contains an $(m-2)$-DOF subrobot's inertia matrix by Lemma 2. Hence, it follows by induction that serial-chain

inertia matrices are recursively cyclic. Note that this proof depends on a relative coordinate system, so Theorem 2 always holds modulo a coordinate transformation. ■

Corollary 1: For any fully actuated n-DOF serial-chain robot with a potential energy that is cyclic in the first k coordinates, there exists a feedback control law that shapes the system to the k-almost-cyclic form, where $1 \leq k < n$, allowing a k-stage controlled reduction by Theorem 1.

Theorem 2 provides the symmetries for k stages of functional Routhian reduction. Each stage divides out a cyclic variable and thus a top-left row-column of the inertia matrix, leaving a new cyclic variable to be divided. After k stages of reduction, the corresponding $(n-k)$-DOF subrobot remains. Moreover, the dynamics of a robot are invariant under translations of the inertial frame[2], so we can redefine each subrobot's inertial frame after a reduction. Therefore previous links can be effectively removed from the dynamics of a subrobot.

By utilizing a reduction-based control law, initial conditions satisfying (17) allow the shaped dynamics of a serial-chain n-DOF robot to project onto the dynamics of the corresponding $(n-k)$-DOF subrobot, which is entirely decoupled from the first k coordinates and thus behaves and can be controlled as a typical $(n-k)$-DOF robot. Moreover, the dynamics of the first k DOF evolve according to momentum constraint (18), showing that the subsystem dynamics do affect the first k coordinates but in a controlled manner. In particular, we can force these coordinates to set-points or periodic orbits with our choice of functional momentum maps $\lambda(q_j) = -\alpha_j(q_j - \bar{q}_j)$, where α_j is a gain constant and $\bar{q}_j$ is a desired angle constant, for $j \in \{1, k\}$. This harnesses natural momentum effects, rather than canceling them as would a naive plant-inversion scheme. It is well-known that natural nonlinearities can be beneficial to control and stability (Krstic et al., 1995), and we see that this is indeed the case here.

At this point, it is important to revisit the assumption that the potential energy is cyclic in the first k coordinates. In many cases, including our biped application, the robot's potential energy will not have the necessary cyclicities to apply Corollary 1. However, we can use potential shaping control[3] to eliminate any potential energy dependence on the variables we wish to reduce, i.e., we impose a "controlled symmetry," thus satisfying the assumptions of Corollary 1. This fact leads to the more general reduction-based control result below.

Corollary 2: For any fully actuated n-DOF serial-chain robot, there exists a feedback control law that shapes the system to the k-almost-cyclic form, where $1 \leq k < n$, allowing a k-stage controlled reduction by Theorem 1.

We now present the application of reduction-based control to bipedal walking robots.

[2]Invariance of the dynamics follows from the fact that the kinetic energy is constructed from the end-effector's body velocity, which is independent of the choice of inertial frame, and the fact that the potential energy is constructed from each link's height function, which under inertial frame translation is offset by constants that disappear after differentiation (Murray et al., 1994).

[3]This is often accomplished with a control law that simply replaces the original potential energy with the potential energy of the target subsystem (which can be found by appropriately fixing the variables to be reduced). We do exactly this for our biped application in Section V.

IV. Bipedal Walking Robots

A simple bipedal walking robot has two phases, a swing phase and a double-support/impact phase, and thus is modeled by a hybrid system. In three dimensions, non-trivial feet introduce one to three degrees of underactuation at the point of contact between the foot and ground, so we assume that the biped has flat feet with full actuation at the stance ankle. During the swing phase, the contact between the flat foot and ground is assumed to be without slipping.[4] We additionally assume that foot impacts are instantaneous and perfectly plastic. Since knee-lock impacts introduce another level of complexity to the hybrid model, we model foot-ground impacts as the only discrete events. This does not necessarily preclude knees without impacts (Grizzle et al., 2001), but the general case with knee-lock impacts is left to future work. We now discuss hybrid systems so that we can construct this paper's model of interest, partially adopting the notation and formalisms developed by Ames et al. in (Ames et al., 2006), (Ames and Gregg, 2007), (Ames et al., 2007).

A. Hybrid Systems

Hybrid systems are dynamical systems containing both continuous and discrete dynamics. Since we are considering simple hybrid systems with one continuous phase, we use the notion of "systems with impulse effects," as in (Grizzle et al., 2001) and (Westervelt et al., 2003), instead of more general hybrid system tuples of terms.

Definition 4: A *hybrid control system* has the form

$$\mathscr{HC}: \begin{cases} \dot{x} = f(x) + g(x)u & x \in D \backslash G \\ x^+ = \Delta(x^-) & x^- \in G \end{cases},$$

where $G \subset D$ is called the *guard* and $\Delta : G \to D$ is the *reset map*. In our context, state $x = (q^T, \dot{q}^T)^T$ is in domain $D \subseteq T\mathcal{Q}$, and we assume full actuation so that control input u is within control space $U \subseteq \mathbb{R}^n$. We describe uncontrolled systems and closed-loop systems by a *hybrid system*, which has no explicit control input u:

$$\mathscr{H}: \begin{cases} \dot{x} = f(x) & x \in D \backslash G \\ x^+ = \Delta(x^-) & x^- \in G \end{cases}.$$

Finally, a *hybrid flow* is a solution to a hybrid system $\mathscr{H}$.

We also must define periodicity, since bipedal walking gaits correspond to periodic orbits of hybrid systems. For example, hipped bipedal walking gaits correspond to 2-step periodic orbits due to natural side-to-side swaying and turning motions. Letting $x(t)$ be a hybrid flow of $\mathscr{H}$, it is k-periodic if $x(t) = x(t + \sum_{i=1}^{k} T_i)$, for all $t \geq 0$, where T_i is the fixed *time to impact* between the $(i-1)^{th}$ and i^{th} discrete events. A k-periodic hybrid flow $x(t)$ is associated with its *k-periodic hybrid orbit* $\mathcal{O} \subset D$, defined as $\mathcal{O} = \{x(t) | t \geq 0\}$.

Local exponential stability of a k-periodic hybrid orbit is defined in the usual manner and determined by studying the corresponding *Poincaré map* $P : G \to G$, as done in (Chevallereau et al., 2008), (Ames et al., 2007). The casual

[4]Note that these assumptions are justified for an approximation of feet that lie flat on the ground with sufficient friction during the entirety of each swing phase. All such assumptions on biped dynamics are common in the literature on passive dynamic walking.

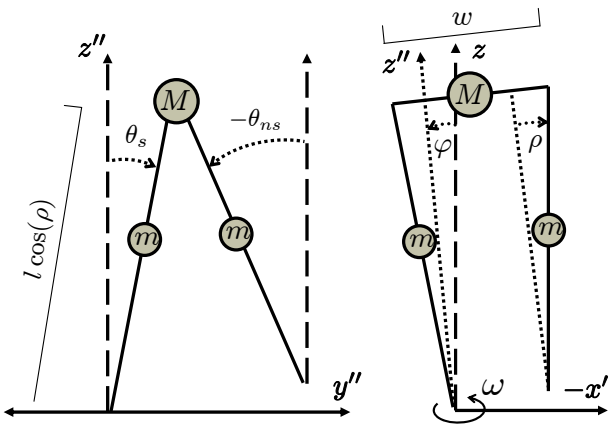

Fig. 2. The sagittal (left) and frontal (right) planes of a hipped 3-D bipedal robot. Note that leg splay angle ρ is a constant modeling parameter.

reader need only know that this is a discrete map defined on the *Poincaré section*, naturally chosen to be guard G, which characterizes the evolution of a hybrid flow between intersections with G. In particular, the k-composition of this map sends state $x_j \in G$ ahead k discrete events by the discrete system $x_{j+k} = P^k(x_j)$. In the case of a k-periodic hybrid orbit $\mathcal{O}$, we have a *k-fixed point* $x^* \in G \cap \mathcal{O}$ such that $x^* = P^k(x^*)$. Although we cannot analytically calculate this map to determine its stability about x^*, we can numerically approximate it through simulation, allowing us to analyze orbit stability by the map's linearization, δP^k. Based on discrete linear system theory, we then know that a k-periodic hybrid orbit is locally exponentially stable if and only if the eigenvalue magnitudes of δP^k are strictly within the unit circle. We defer the numerical details to (Goswami et al., 1996).

B. Four-DOF Biped Model

We now construct the model of a 4-DOF bipedal robot with a hip and splayed legs (Fig. 2). Although this is a 3-D extension of the 2-D compass-gait biped seen in the sagittal plane of Fig. 2, it is important to note that the 3-D model does not have stable passive walking gaits down slopes. We, therefore, will use reduction-based control on this serial-chain robot to construct pseudo-passive 3-D walking gaits from the sagittal plane. This model's hybrid control system is

$$\mathscr{HC}_{\,4\mathrm{D}} : \begin{cases} \dot{x} = f_{4\mathrm{D}}(x) + g_{4\mathrm{D}}(x)u & x \in D_{4\mathrm{D}} \backslash G_{4\mathrm{D}} \\ x^+ = \Delta_{4\mathrm{D}}(x^-) & x^- \in G_{4\mathrm{D}} \end{cases} .$$

The configuration space for the 4-DOF biped can be represented by $Q_{4\mathrm{D}} = SO(3) \times \mathbb{S}^1$ (Spong and Bullo, 2005). In particular, 3×3-matrix $R_s \in SO(3)$ is the orientation of the stance leg and $\theta_{ns} \in \mathbb{S}^1$ is the relative shape the nonstance/swing leg. However, before we obtain the equations of motion, we must parameterize the configuration space $Q_{4\mathrm{D}}$. An element of $SO(3)$ can be minimally represented by an ordered set of three ZYX Euler angles[5] $(\omega, \varphi, \theta_s) \in \mathbb{T}^3$, which correspond to the yaw, roll, and pitch angles of the stance leg (and are the robot's first three

[5]Note that this local parameterization's singularity is at $\varphi = -\pi/2$, which corresponds to an irrelevant fall configuration.

DOF). For the sake of distinguishing the sagittal-plane configuration, we take $Q_{4\mathrm{D}} = \mathbb{T}^2 \times \mathbb{T}^2$, with coordinates $q = (\omega, \varphi, \theta^T)^T$, where ω is the yaw (or heading), φ is the roll (or lean) from vertical, and $\theta = (\theta_{\mathrm{s}}, \theta_{\mathrm{ns}})^T$ is the vector of sagittal-plane (pitch) variables as in the 2-D compass-gait model. All other parameters, including leg splay angle ρ, are held constant.

We derive the continuous dynamics for $\mathscr{HC}_{4\mathrm{D}}$ using the previously described method. We start with Lagrangian

$$L_{4\mathrm{D}}(q, \dot{q}) = \frac{1}{2}\dot{q}^T M_{4\mathrm{D}}(q)\dot{q} - V_{4\mathrm{D}}(q),$$

with recursively-cyclic 4×4 inertia matrix (see Appendix C for the symbolic terms)

$$\begin{aligned} M_{4\mathrm{D}}(\varphi, \theta) &= \begin{pmatrix} m_\omega(\varphi,\theta) & M_{\omega,\varphi,\theta}(\varphi,\theta) \\ M^T_{\omega,\varphi,\theta}(\varphi,\theta) & M_{3\mathrm{D}}(\theta) \end{pmatrix} \\ &= \begin{pmatrix} m_\omega(\varphi,\theta) & \text{—} & M_{\omega,\varphi,\theta}(\varphi,\theta) \\ | & m_\varphi(\theta) & M_{\varphi,\theta}(\theta) \\ M^T_{\omega,\varphi,\theta}(\varphi,\theta) & M^T_{\varphi,\theta}(\theta) & M_\theta(\theta) \end{pmatrix} \end{aligned}$$

and potential energy

$$V_{4\mathrm{D}}(\varphi, \theta) = V_\theta(\theta)\cos(\varphi) - \frac{g}{2}(2m + M)(w - 2l\sin(\rho))\sin(\varphi), \tag{19}$$

which contains the planar subsystem potential energy

$$V_\theta(\theta) = \frac{gl}{2}\cos(\rho)((3m + 2M)\cos(\theta_s) - m\cos(\theta_{ns})). \tag{20}$$

The dynamical equations of motion for the fully actuated walker are then

$$M_{4\mathrm{D}}(q)\ddot{q} + C_{4\mathrm{D}}(q, \dot{q})\dot{q} + N_{4\mathrm{D}}(q) = B_{4\mathrm{D}}u, \tag{21}$$

where $C_{4\mathrm{D}}$ and $N_{4\mathrm{D}}$ are defined as usual and with invertible 4×4-matrix

$$B_{4\mathrm{D}} = \begin{pmatrix} I_{2\times 2} & 0_{2\times 2} \\ 0_{2\times 2} & B_\theta \end{pmatrix} \text{ with } B_\theta = \begin{pmatrix} 1 & 1 \\ 0 & -1 \end{pmatrix}.$$

These dynamics are associated with the control system $(f_{4\mathrm{D}}, g_{4\mathrm{D}})$ with input u. We model actuator saturation at torque constant U_{max}, so the control space is $U_{4\mathrm{D}} = \{u \in \mathbb{R}^4 : |u_i| \leq U_{max}, \forall i \in \{1, 4\}\}$.

In order to appropriately model walking on a flat surface, we introduce a unilateral constraint function representing the height of the swing foot[6]:

$$H_{4\mathrm{D}}(q) = l\cos(\rho)(\cos(\theta_s) - \cos(\theta_{ns}))\cos(\varphi) - (w - 2l\sin(\rho))\sin(\varphi).$$

States corresponding to feasible walking configurations live in domain $D_{4\mathrm{D}}$, the subset of $TQ_{4\mathrm{D}}$ where this height is nonnegative. Impact events are triggered by intersections with the guard, $G_{4\mathrm{D}} \subset D_{4\mathrm{D}}$, where the height of the

[6]The yaw-DOF (coordinate ω) is about the vertical axis, and thus the height of the foot $H_{4\mathrm{D}}(q)$, measured across this vertical axis, is invariant under such rotations.

swing foot is zero and decreasing (to exclude events associated with scuffing):

$$G_{4\mathrm{D}} = \left\{ \begin{pmatrix} q \\ \dot{q} \end{pmatrix} \in D_{4\mathrm{D}} : H_{4\mathrm{D}}(q) = 0 \text{ and } \dot{H_{4\mathrm{D}}}(q) = \left(\frac{\partial H_{4\mathrm{D}}(q)}{\partial q} \right)^T \dot{q} < 0 \right\}.$$

Following the method of (Grizzle et al., 2001), we derive the reset map associated with the impact equations:

$$\Delta_{4\mathrm{D}}(q, \dot{q}) = \begin{pmatrix} \Gamma_{4D} q \\ \Omega_{4D}(q)\dot{q} \end{pmatrix}, \tag{22}$$

where angular velocity map[7] $\Omega_{4D}(q) \in \mathbb{R}^{4\times 4}$ and angular position map

$$\Gamma_{4D} = \begin{pmatrix} I_{2\times 2} & 0_{2\times 2} \\ 0_{2\times 2} & \Gamma_\theta \end{pmatrix} \text{ with } \Gamma_\theta = \begin{pmatrix} 0 & 1 \\ 1 & 0 \end{pmatrix}.$$

The signs of w and ρ are flipped at impact to model the change in stance leg. Technically the hybrid model should then have two sets of continuous/discrete phases, but we forgo this caveat for simplicity and note that the system should be 2-periodic. We now construct a reduction-based control law for this robot.

V. The Control Law

In the multistage controlled reduction result of Corollary 2, the controller is designed to recursively break cyclic symmetries in the special almost-cyclic manner. The inner loop of the control law shapes the energy of our robot to the 2-almost-cyclic form, and the nested outer loop plays two roles:

1) Implements passivity-based control on the reduced 2-D-subsystem to construct robust flat-ground gaits.
2) Stabilizes to a surface defined by constraint (18) so that Theorem 1 holds.

This builds upon the construction of the single-stage control law from (Ames et al., 2007). As mentioned earlier, we will model actuator saturation to demonstrate this method's practicality. We ignore saturation during the control law derivation, but simulations will show that it is indeed robust to clipping effects. We begin by describing the Lagrangian-shaping inner loop.

A. Lagrangian Shaping Controller

This controller uses kinetic and potential energy shaping to transform $L_{4\mathrm{D}}$ to the 2-almost-cyclic form for controlled reduction to the biped's planar subsystem. Given configuration vector $q = (\omega, \varphi, \theta^T)^T$, the 4-DOF potential $V_{4\mathrm{D}}$ of (19) is clearly not cyclic in the second variable φ, and thus we must make it so by imposing a "controlled symmetry" with respect to the second coordinate's rotation group $\mathbb{S}^1$. This is most naturally accomplished with potential shaping to replace $V_{4\mathrm{D}}$ with V_θ of (20), the planar walker's cyclic potential energy (constructed from a scaled height due to splay angle ρ). We will incorporate this shaping into the control law.

We begin with the generalized ACL of (4a) for $k = 2$, $n = 4$:

$$L_{\lambda_1^2}(q, \dot{q}) \quad = \quad \frac{1}{2}\dot{q}^T M_{\lambda_1^2}(q_2^4)\dot{q} + Q_{\lambda_1^2}^T(q)\dot{q} - V_{\lambda_1^2}(q),$$

[7]This map's complexity prevents a closed-form symbolic derivation in Mathematica, so this is computed numerically at each impact event.

where $M_{\lambda_1^2}$, $Q_{\lambda_1^2}$ and $V_{\lambda_1^2}$ are defined by substituting $M_{4\mathrm{D}}$ for M and V_θ for V_{fct} in (6)-(8). Direct calculation shows that the stage-2 functional Routhian associated with 2-ACL $L_{\lambda_1^2}$ is the Lagrangian of the scaled planar walker:

$$L_{2\mathrm{D}}(\theta, \dot{\theta}) = \frac{1}{2}\dot{\theta}^T M_\theta(\theta)\dot{\theta} + V_\theta(\theta),$$

which yields the reduced control system $(f_{2\mathrm{D}}, g_{2\mathrm{D}})$ with subsystem input v_θ.

Given this target reduction, the control law that shapes L into $L_{\lambda_1^2}$ and allows auxiliary control is

$$u := B_{4\mathrm{D}}^{-1}\left(C_{4\mathrm{D}}(q,\dot{q})\dot{q} + N_{4\mathrm{D}}(q) + M_{4\mathrm{D}}(\varphi,\theta)M_{\lambda_1^2}(\varphi,\theta)^{-1}\left(-C_{\lambda_1^2}(q,\dot{q})\dot{q} - N_{\lambda_1^2}(q) + B_{4\mathrm{D}}v\right)\right), \tag{23}$$

where $C_{\lambda_1^2}$ and $N_{\lambda_1^2} = \frac{\partial}{\partial q}V_{\lambda_1^2}$ are the shaped terms as in (9), and the vector $v = (v_\omega, v_\varphi, v_\theta^T)^T$ contains the auxiliary control inputs to be defined. Finally, using momentum map functions $\lambda_1(\omega) = -\alpha_1(\omega - \bar{\omega})$ and $\lambda_2(\varphi) = -\alpha_2\varphi$, for $\alpha_1, \alpha_2 > 0$, we establish directional control to constant angle $\bar{\omega}$ for the yaw/heading DOF and lateral correction to vertical for the roll/lean DOF. Inputting (23) into biped control system $(f_{4\mathrm{D}}, g_{4\mathrm{D}})$, we have the shaped dynamics

$$M_{\lambda_1^2}(\varphi,\theta)\ddot{q} + C_{\lambda_1^2}(q,\dot{q})\dot{q} + N_{\lambda_1^2}(q) = B_{4\mathrm{D}}v,$$

which project onto the target dynamics of the scaled planar biped. We associate the full-order shaped dynamics with the new control system $(f_{\lambda_1^2}, g_{\lambda_1^2})$ as in (10), with control input v to be defined next.

B. Subsystem Passivity-Based Controller

Since we can decouple the robot's last two degrees-of-freedom (the reduced subsystem), we can control it as a planar 2-DOF biped with well-known passivity-based techniques in v_θ. The first of these techniques is that of slope-changing "controlled symmetries," which will allow our biped to walk on flat ground given planar walking cycles down slopes (Spong, 1999), (Spong and Bullo, 2005).

In three dimensions, the orientation of the ground (the slope) can be represented by a rotation of the world frame, i.e., an element of $SO(3)$. Thus, any change of slope is characterized by a group action of $SO(3)$ on our bipedal walker's configuration space $Q_{4\mathrm{D}}$:

$$\Phi_A(R_s, \theta_{ns}) = (A \cdot R_s, \theta_{ns}), \;\; A \in SO(3).$$

The behavior of a passive biped strongly depends on the ground slope. Although both the kinetic energy and impact events are invariant under the slope changing action Φ, this is not the case for the potential energy (Spong and Bullo, 2005). We can, however, control the robot's potential to the desired world orientation and thus impose symmetry on the system, i.e., a *controlled symmetry*. With such a symmetry, any stable limit cycle down a slope can be mapped to a stable limit cycle on an arbitrary slope.

For the sagittal-plane compass-gait biped, stable passive/uncontrolled limit cycles exist down shallow slopes between about 3° and 5°, as shown in (McGeer, 1990), (Goswami et al., 1996). This is the range of slope angles for which the potential energy introduced by gravity over each stride is matched by the energy dissipated at foot impact with ground. For this planar robot,

$$\Phi_A(\theta) = \theta + \beta = (\theta_s + \beta, \theta_{ns} + \beta)^T,$$

where $\beta = \sigma - \delta$ is the angle of rotation parameterizing $A \in SO(2)$, σ is the slope angle yielding the desired passive limit cycle (such as $\pi/50$), and δ is the actual ground slope angle for controlled "pseudo-passive" walking. Since our 4-DOF biped's forward walking motion is dominated by its sagittal plane, we want to implement controlled symmetries on this 2-D subsystem to construct full-order gaits on flat ground ($\delta = 0$), and the control that achieves the desired gait mapping is

$$v_\theta^\beta = B_\theta^{-1} \frac{\partial}{\partial \theta} \left(V_\theta(\theta) - V_\theta(\theta + \beta) \right), \quad \beta = \frac{\pi}{50}.$$

As for the robustness of this desired subsystem limit cycle, each impact event will amplify any perturbations in several dimensions. This is especially an issue when the biped is turning, as these maneuvers inherently deviate from full-order straight-walking limit cycles and thus threaten the planar subsystem's stability. In order to increase overall robustness, we implement passivity-based constant-energy tracking from (Spong, 2004) on this critical 2-D subsystem (which has a nearly constant energy in our hipped case).

To begin, we define the Lyapunov-like storage function

$$S = \frac{1}{2}(E_{2D} - E_{2D}^{ref})^2 \geq 0,$$

where E_{2D}^{ref} is a constant reference energy and E_{2D} is the 2-D-subsystem energy after controlled symmetries:

$$\begin{aligned} E_{2D} &= K_\theta + V_\theta^\beta \\ &= K_\theta + V_\theta + (-V_\theta + V_\theta^\beta), \end{aligned} \tag{24}$$

with $K_\theta = \frac{1}{2}\dot{\theta}^T M_\theta(\theta)\dot{\theta}$ and $V_\theta^\beta = V_\theta(\theta + \beta)$.

Due to the passivity property of robots, we have

$$\dot{E_{2D}} = \dot{\theta}^T \left(B_\theta v_\theta - \frac{\partial V_\theta}{\partial \theta} + \frac{\partial V_\theta^\beta}{\partial \theta} \right)$$

along trajectories of the shaped system. And, using passivity-based control on the 2-D subsystem:

$$v_\theta := v_\theta^\beta + \tilde{v}_\theta = B_\theta^{-1} \left(\frac{\partial V_\theta}{\partial \theta} - \frac{\partial V_\theta^\beta}{\partial \theta} \right) + \tilde{v}_\theta, \tag{25}$$

it follows that $\dot{E_{2D}} = \dot{\theta}^T \tilde{v}_\theta$. Then, taking the derivative of the storage function yields $\dot{S} = (E_{2D} - E_{2D}^{ref})\dot{\theta}^T \tilde{v}_\theta$.

If we wisely choose the auxiliary input $\tilde{v}_\theta$ for energy tracking, such as feedback law

$$\tilde{v}_\theta = -B_\theta^{-1} p (E_{2D} - E_{2D}^{ref}) \dot{\theta} \tag{26}$$

with $p > 0$, then we have the negative semidefinite

$$\dot{S} = -2p||\dot{\theta}||^2 S \leq 0.$$

It is proven in (Spong, 2004) that under reasonable conditions (including control input saturation), this implies exponential convergence of a planar biped's total energy to the reference energy between step impacts. If the reference is chosen to be the constant energy corresponding to a stable limit cycle (assuming that the limit cycle has nearly constant energy), then this passivity-based controller expands the limit cycle's basin of attraction.

The subsystem control law (25) is incorporated into the full-order shaped system ($f_{\lambda_1^2}$,$g_{\lambda_1^2}$) by defining the new control system ($\hat{f}_{\lambda_1^2}$,$\hat{g}_{\lambda_1^2}$) with input $v_1^2 = (v_\omega, v_\varphi)^T$ as in (11). Similarly, the 2-reduced, v_θ-controlled vector field $\hat{f}_{2\mathrm{D}}$ is defined as in (16). In order to ensure the decoupling of $\hat{f}_{2\mathrm{D}}$ by Theorem 1, we now design control law v_1^2 to enforce constraint (18).

C. Zero Dynamics Controller

The beneficial implications of Theorem 1 only hold from the limited set of states satisfying (17), so we must use control outside of this set to exploit the controlled reduction result. Therefore, we extend the approach and notation of (Ames and Gregg, 2007) in using output linearization to force trajectories toward states satisfying constraints (18). We first define output functions corresponding to the error from these desired constraints:

$$h_i(q_i^4, \dot{q}_i^4) := \dot{q}_i - \frac{1}{m_{q_i}(q_{i+1}^4)} \left(\lambda_i(q_i) - M_{q_i, q_{i+1}^4}(q_{i+1}^4) \dot{q}_{i+1}^4 \right),$$

for $i \in \{1, 2\}$.

We design the control law to zero these two output functions in our MIMO nonlinear control system by the method discussed in (Sastry, 1999). In other words, we want to stabilize the "zero dynamics" surface

$$\mathcal{Z} = \left\{ \begin{pmatrix} q \\ \dot{q} \end{pmatrix} \in T\mathcal{Q} : h_i(q_i^4, \dot{q}_i^4) = 0, \ \ \forall i \in \{1, 2\} \right\}.$$

To do this, we must define the 2×2-matrix of Lie derivatives with respect to $\hat{g}_{\lambda_1^2}$:

$$A(q) = \begin{pmatrix} \frac{\partial h_1(q,\dot{q})}{\partial q} & \frac{\partial h_2(q_2^4,\dot{q}_2^4)}{\partial q} \end{pmatrix}^T \hat{g}_{\lambda_1^2}(q),$$

of which element $A_{i,j}$ is $L_{\hat{g}_{\lambda_1^2} e_j} h_i$, the Lie derivative of h_i with respect to $\hat{g}_{\lambda_1^2} e_j$, where e_j is the j^{th} standard basis vector of $\mathbb{R}^2$. Also, $A(q)$ is positive-definite, since $L_{\hat{g}_{\lambda_1^2} e_i} h_i(q_i^4, \dot{q}_i^4) = \frac{1}{m_{q_i}(q_{i+1}^4)}$, where $m_{q_i}(q_{i+1}^4) > 0$ by the positive-definite inertia matrix property of $M_{4\mathrm{D}}(q)$.

Then, the control law that achieves the desired behavior is

$$v_1^2 := -A(q)^{-1} \left(\begin{pmatrix} L_{\hat{f}_{\lambda_1^2}} h_1(q, \dot{q}) \\ L_{\hat{f}_{\lambda_1^2}} h_2(q_2^4, \dot{q}_2^4) \end{pmatrix} + \begin{pmatrix} \xi_1 & 0 \\ 0 & \xi_2 \end{pmatrix} \begin{pmatrix} h_1(q, \dot{q}) \\ h_2(q_2^4, \dot{q}_2^4) \end{pmatrix} \right), \tag{27}$$

where $L_{\hat{f}_{\lambda_1^2}} h_i$ is the Lie derivative of h_i with respect to $\hat{f}_{\lambda_1^2}$, and $\xi_i > 0$ is a new "proportional" control gain, for $i \in \{1, 2\}$. It is clear that v_1^2 is well-defined by the positive-definiteness of $A(q)$ and the control gain matrix. And finally, $v_1^2\big|_{\mathcal{Z}} = 0$, so this controller does not interfere with Theorem 1 when on surface $\mathcal{Z}$.

VI. Simulations

We now examine our 4-DOF biped, introduced in Section IV, with physical parameters shown in Table I. In order to walk straight-forward using reduction-based control law (23), we choose a tight momentum map λ_1, with gain constant $\alpha_1 = 15$ and desired heading $\bar{\omega} = 0$, to counteract the yaw motion induced by the hip. The other control parameters are also given in Table I. Applying (23) under saturation constant $U_{max} = 20$ Nm, the hybrid

TABLE I

4-DOF BIPED MODEL

Physical Parameters	Hip Mass	Leg Mass	Hip Width	Leg Length	Leg Splay Angle	Saturation Constant
Variable	M	m	w	l	ρ	U_{max}
Value	10 kg	5 kg	0.1 m	1 m	0.0188 rad	20 Nm

Control Parameters	λ_1-Gain	λ_1-Angle	λ_2-Gain	h_1-Gain	h_2-Gain	v_θ^β-Angle	$\tilde{v}_\theta$-Gain	$\tilde{v}_\theta$-Energy
Variable	α_1	$\bar{\omega}$	α_2	ξ_1	ξ_2	β	p	E_{2D}^{ref}
Value	15	0 rad	10	30	15	$\pi/50$ rad	20	154.8742 J

control system $\mathscr{HC}_{4\mathrm{D}}$ yields the closed-loop hybrid system $\mathscr{H}_{4\mathrm{D}}^{\mathrm{cl}}$. Then, assuming that the Lagrangian-shaping and controlled symmetry inputs are within saturation bounds,[8] $\mathscr{H}_{4\mathrm{D}}^{\mathrm{cl}}$ has total 4-DOF energy

$$\begin{aligned} E_{4D} &= \frac{1}{2}\dot{q}^T M_{\lambda_1^2}(\varphi,\theta)\dot{q} + Q_{\lambda_1^2}^T(q)\dot{q} + V_{\lambda_1^2}^\beta(\theta) \\ &= \frac{1}{2}\dot{q}^T M_{\lambda_1^2}(\varphi,\theta)\dot{q} + Q_{\lambda_1^2}^T(q)\dot{q} + V_\theta^\beta(\theta) - \frac{1}{2}\frac{\lambda_1(\omega)^2}{m_\omega(\varphi,\theta)} - \frac{1}{2}\frac{\lambda_2(\varphi)^2}{m_\varphi(\theta)}, \end{aligned}$$

reduced 3-DOF subsystem energy

$$\begin{aligned} E_{3D} &= \frac{1}{2}\begin{pmatrix} \dot{\varphi} & \dot{\theta}^T \end{pmatrix} M_{\lambda_2^2}(\theta)\begin{pmatrix} \dot{\varphi} \\ \dot{\theta} \end{pmatrix} + Q_{\lambda_2^2}^T(\varphi,\theta)\begin{pmatrix} \dot{\varphi} \\ \dot{\theta} \end{pmatrix} + V_{\lambda_2^2}^\beta(\theta) \\ &= \frac{1}{2}\begin{pmatrix} \dot{\varphi} & \dot{\theta}^T \end{pmatrix} M_{3\mathrm{D}}(\theta)\begin{pmatrix} \dot{\varphi} \\ \dot{\theta} \end{pmatrix} + \frac{1}{2}\dot{\theta}^T\frac{M_{\varphi,\theta}(\theta)^T M_{\varphi,\theta}(\theta)}{m_\varphi(\theta)}\dot{\theta} \\ &\qquad - \frac{\lambda_2(\varphi)}{m_\varphi(\theta)}M_{\varphi,\theta}(\theta)\dot{\theta} + V_\theta^\beta(\theta) - \frac{1}{2}\frac{\lambda_2(\varphi)^2}{m_\varphi(\theta)}, \end{aligned}$$

and planar 2-D-subsystem energy E_{2D} as defined in (24). These energy quantities will be relevant to the stability discussion of our biped's walking gaits, particularly when considering the influence of the passivity-based energy-tracking subcontroller.

A. Reduction-Based Control Results

Generally speaking, we cannot analyze the stability of $\mathscr{H}_{4\mathrm{D}}^{\mathrm{cl}}$ using the restricted Poincaré map associated with the reduced 2-D-subsystem. This is because at every impact event, joint velocities encounter a discontinuous jump off the conserved quantity surface $\mathcal{Z}$ (except for the opposing special case of hipless bipeds studied in (Ames and Gregg, 2007) and (Gregg and Spong, 2009a)). Away from this surface, solutions of $\hat{f}_{\lambda_1^2}$ and $\hat{f}_{2\mathrm{D}}$ cannot be analytically related by Theorem 1, so the beneficial decoupling effect for the 2-D-subsystem limit cycle does not hold. We tune zero dynamics law v_1^2 with sufficiently large gains ξ_1, ξ_2 to quickly correct this error during each step cycle, so that any incurred perturbation off the subsystem limit cycle does not leave the basin of attraction (which is expanded by passivity-based law $\tilde{v}_\theta$).

[8] All such assumptions on the control input and its bounds are confirmed in simulation by observing the required torques.

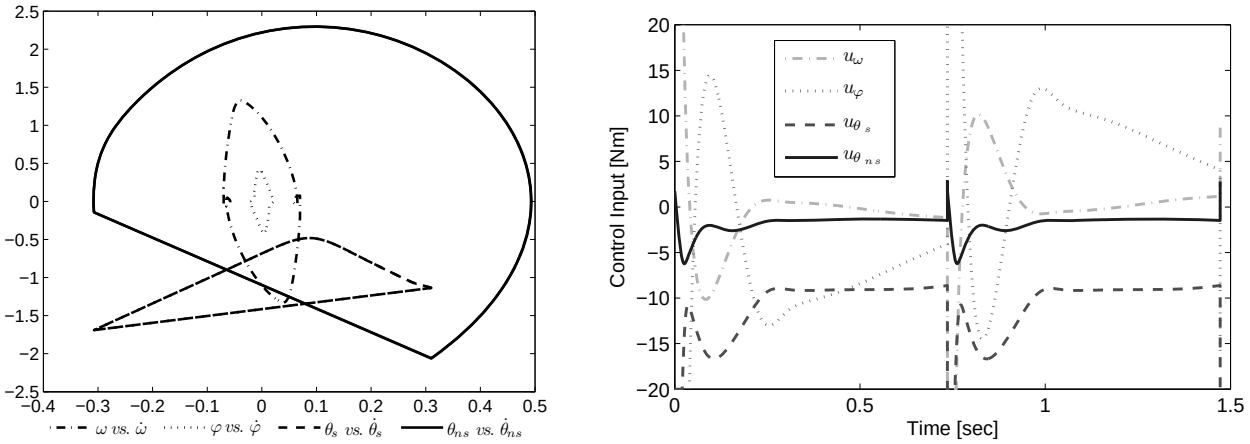

Fig. 3. Phase portrait (left) and saturated control input (right) of the 4-DOF biped's two-step straight-walking cycle.

Therefore, we must consider the full-order behavior of the biped's straight-forward walking gait on flat ground. Simulations in Matlab show that $\mathscr{H}_{4\mathrm{D}}^{\mathrm{cl}}$ produces a 2-periodic limit cycle, $\mathcal{O}_{4\mathrm{D}}$ of Fig. 3, which is constructed from its planar subsystem's limit cycle. The intersection between $\mathcal{O}_{4\mathrm{D}}$ and the Poincaré section over two steps, known as the 2-fixed point, is

$$\begin{pmatrix} q^* \\ \dot{q}^* \end{pmatrix} \approx (0.0699, 0.0135, -0.3074, 0.3102, 0.0774, -0.0508, -1.6907, -2.0610)^T.$$

We numerically calculate the eigenvalue magnitudes of the linearized Poincaré map to be within the unit circle:

$$\{\mathrm{abs}(\mathrm{eig}_i)\} \approx \{0.2047, 0.2047, 0.1286, 0.0383, 0.0037, 0.0000, 0.0000, 0.0000\}, \tag{28}$$

thus confirming that $\mathcal{O}_{4\mathrm{D}}$ is a locally exponentially stable periodic orbit of $\mathscr{H}_{4\mathrm{D}}^{\mathrm{cl}}$. We see in Fig. 3 that the yaw dynamics of the axial plane and the lean dynamics of the frontal plane follow 2-periodic orbits. These motions are naturally induced by the robot's hip during each step cycle (and we verify that these motions disappear when $w = 0, \rho = 0$), but they evolve in a controlled periodic manner due to our choice of functional momentum maps. The clipped input spikes in Fig. 3 are an artifact of subcontrollers (25) and (27) acting to proportionally correct the error in conserved quantities and 2-D-subsystem energy introduced at each impact event. This might raise concern about violating the friction cone at the ground contact point, but input saturation can enforce such constraints. In this paper, we have assumed no slipping, leaving a formal friction analysis to future work.

We now examine gait robustness by perturbing the 2-fixed point corresponding to the biped with passivity-based energy tracking (gain $p = 20$) and the biped without passivity-based energy tracking (gain $p = 0$). Using perturbations $\delta q = 0.01$, $\delta \dot{q} = 0.05$, we simulate six steps and observe the response for each system. In the phase portraits of Fig. 4, we see that the walker begins to fall without energy tracking but recovers nicely with the passivity-based control. Moreover, Fig. 5 shows that the former system is unable to contain the subsystem energies after the perturbation (leading to instability), but the passivity-controlled system sufficiently insulates the subsystem

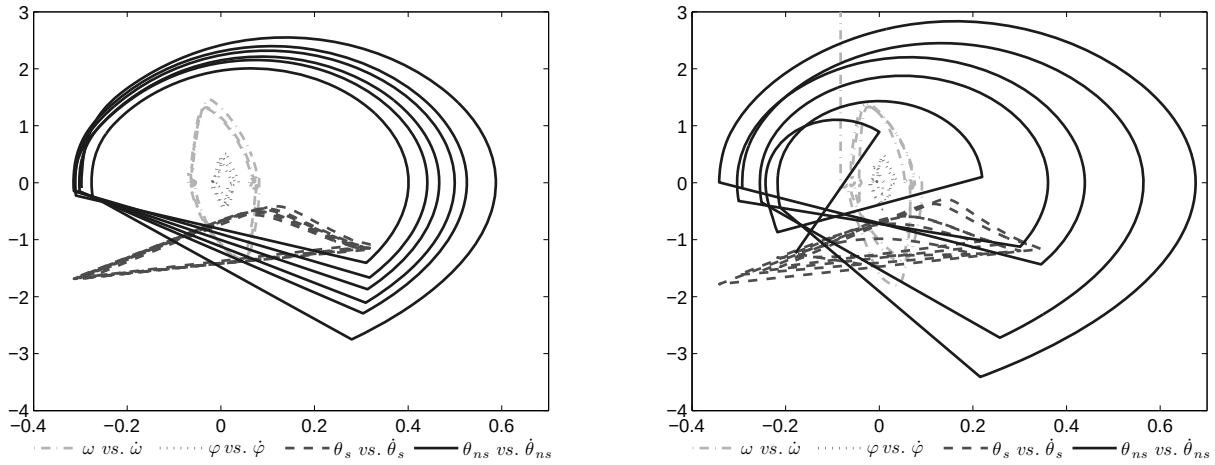

Fig. 4. Perturbed phase of hipped 4-DOF biped with passivity-based energy tracking (left) and without (right).

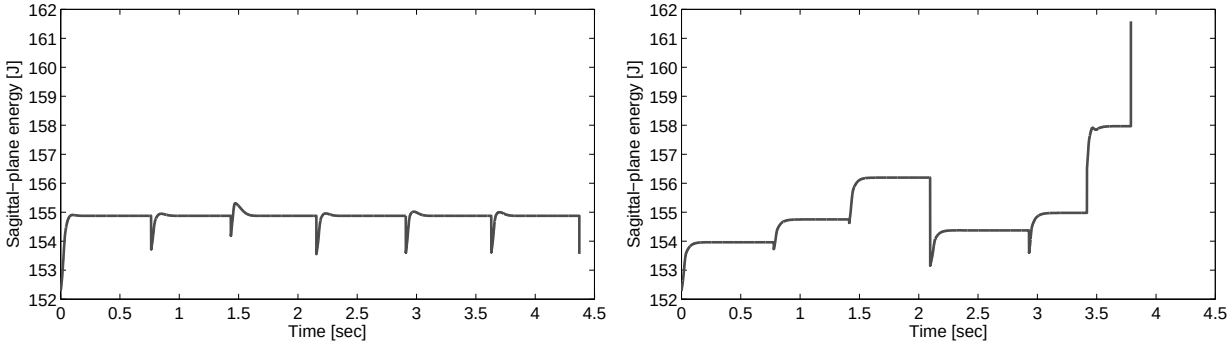

Fig. 5. Perturbed 2D subsystem energies of hipped 4-DOF biped with passivity-based energy tracking (left) and without (right).

energies and allows convergence to the limit cycle. In general, we observe that limit cycle convergence takes far fewer steps when using the passivity-based energy-tracking subcontroller.

In order to demonstrate the directional capabilities of this controlled 4-DOF walker, we instruct the biped to perform a 90° turn over several steps. This is done by starting with $\bar{\omega} = 0$, and at every other step incrementing the desired yaw angle by $\pi/10$ until $\bar{\omega} = \pi/2$. The turning maneuver and required torques are shown in Fig. 6 with the phase in Fig. 7. We see in Fig. 7 that the zero dynamics subcontroller corrects the conserved quantities between each step. The passivity-based control also keeps the sagittal subsystem energy E_{2D} at the desired level, despite the injected energy from yaw rotation. Once the biped meets desired heading $\bar{\omega} = \pi/2$, its gait stably converges to the straight-walking 2-periodic limit cycle of $\mathcal{O}_{4\mathrm{D}}$ with a horizontally-shifted yaw orbit. For this example, we are not considering dynamic stability in the classical sense, since turning maneuvers inherently deviate from limit cycles. Therefore, we say the controlled biped is *robust* through this successful maneuver.

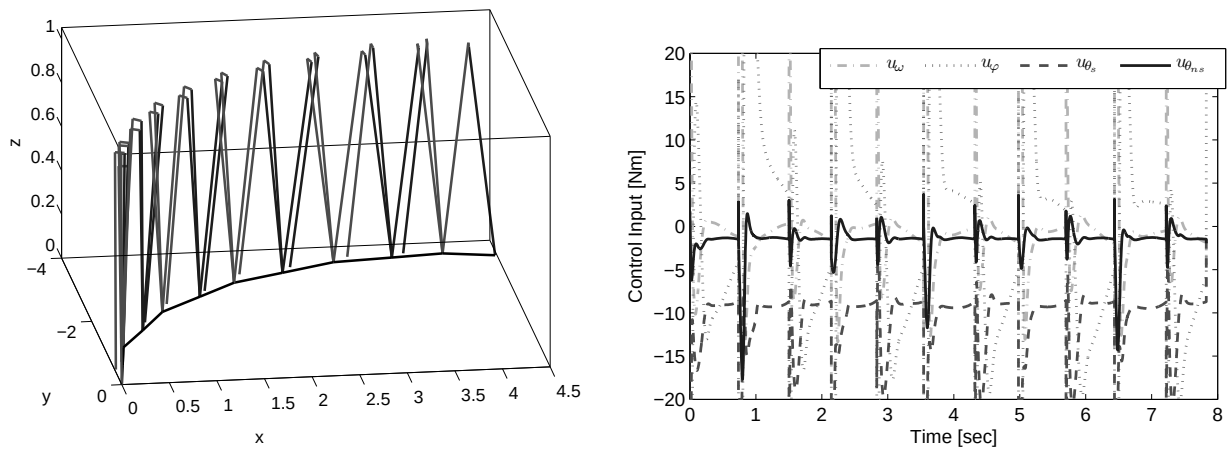

Fig. 6. A 90°-turning maneuver (left) and saturated control (right) for the 3-D hipped 4-DOF biped.

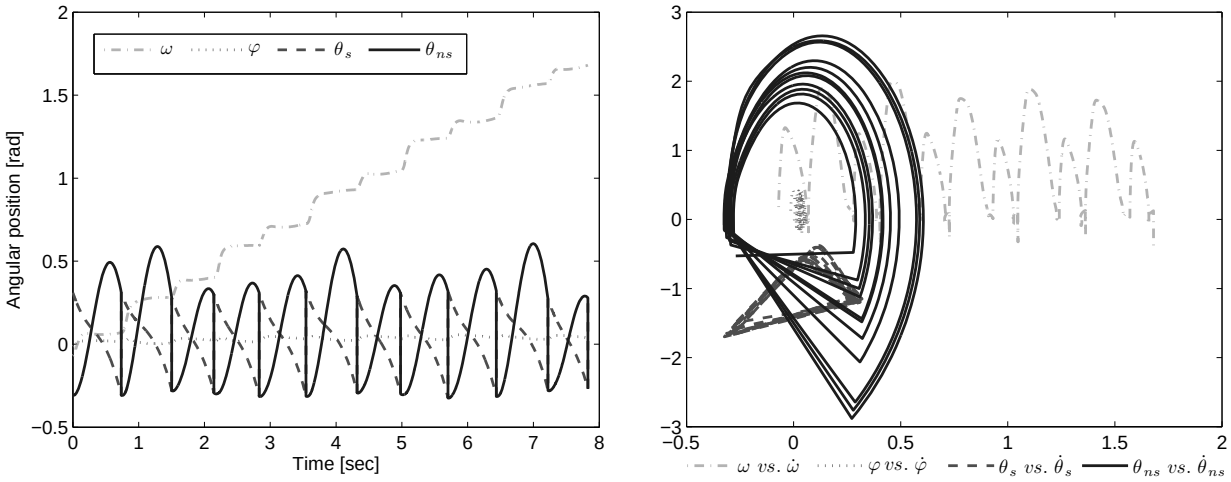

Fig. 7. Configuration trajectories (left) and phase portrait (right) of the hipped 4-DOF biped's 90°-turning maneuver.

B. Compared to Feedback Linearization Methods

The benefits of the controlled reduction method are apparent with such turning maneuvers, but given our assumption of full actuation, one might instead consider making the entire system linear using plant inversion. After all, with large enough gains one could conceivably control the biped to any walking gait. However, since the input torques are saturated, we cannot replace the plant with arbitrary dynamics. Impact events introduce velocity discontinuities according to map (22), which in most cases will jump off the desired limit cycle. Because we cannot use huge gains, we cannot control the biped to arbitrary trajectories during the limited time between impacts. The notion of tracking arbitrary limit cycles may be infeasible, but we might consider partial feedback linearization to take advantage of 2-D-subsystem limit cycles as we do in the presented reduction framework.

We now examine a controller that linearizes the yaw dynamics about desired heading angle $\bar{\omega}$ and the lean dynamics about vertical. Moreover, this law uses feedback cancelation to decouple the planar subsystem, in order

to produce flat-ground walking gaits based on passive 2-D dynamics. Thus, the desired closed-loop dynamics are

$$\begin{aligned} \ddot{\omega} + k_\omega^d \dot{\omega} + k_\omega^p(\omega - \bar{\omega}) &= 0 \\ \ddot{\varphi} + k_\varphi^d \dot{\varphi} + k_\varphi^p \varphi &= 0 \\ M_\theta(\theta)\ddot{\theta} + C_\theta(\theta, \dot{\theta})\dot{\theta} + N_\theta^\beta(\theta) &= 0, \end{aligned}$$

but as we just discussed, these decoupled dynamics will not hold while the control input is clipping.

Using this control method, we do find straight-forward walking gaits based on the 2-D-subsystem, although the natural side-to-side swaying motions are almost entirely canceled. This is not surprising, as we are essentially replacing the 4-DOF hipped biped's dynamics with that of a planar hipless biped and two decoupled linear PD systems, all of which are known to be stable. However, when we instruct this controlled biped to perform a 90° turn as before, it fails. Choosing small critically-damped PD gains, $k_\omega^p = 5$, $k_\varphi^p = 20$, $k_\omega^d = 2\sqrt{k_\omega^p}$, $k_\varphi^d = 2\sqrt{k_\varphi^p}$, the biped makes loose sloppy turns and eventually trips (Fig. 8). With large critically-damped gains, $k_\omega^p = 150$, $k_\varphi^p = 250$, etc., we see immediate failure in Fig. 9 – the quick turning motion destabilizes the sagittal-plane limit cycle, causing a strange backwards misstep and subsequent fall. The inputs for both cases are shown in Fig. 10.

We see that feedback linearization/decoupling is sufficient for straight-forward walking, when the actual hipped dynamics are closer to the desired planar hipless dynamics, but this method is not robust for highly dynamic motions like turning, when the hip induces a strong coupling between the yaw, lean, and pitch modes. We have no guarantees on hybrid stability off the reference limit cycle, because the decoupling of the critical 2-D subsystem is violated by impacts and input saturation. On the other hand, controlled reduction maintains the decoupling of this subsystem from anywhere on the conserved quantity surface $\mathcal{Z}$, resulting in a much larger set of robust states.

VII. Conclusions

These results show that a completely 3-D bipedal robot can achieve stable directional walking with a saturated reduction-based control law. This method requires only the existence of stable limit cycles in the sagittal subsystem, thus simplifying the search for full-order stable limit cycles and expanding the class of walking robots that can stably exploit passive dynamics in three dimensions. Controlled reduction embraces the beneficial passive dynamics of the robot, so the required torques are feasible and the resulting dynamic walking gaits appear natural with human-like swaying motion. We have a reasonable understanding of limit cycle stability, since the high-dimensional basin of attraction depends primarily on the sagittal-plane subsystem, for which locally stable behavior is guaranteed from anywhere on the conserved quantity surface. And because we do not enforce a particular trajectory, overall walking gaits need not be known a priori, suggesting a natural robustness to environmental variability.

This form of controlled reduction is presented in the general k-stage case, so this method easily extends to higher-dimensional systems. However, this theory concerns fully-actuated serial-chain robots, precluding application to robots with feet, torsos, or arms. Controlled reduction is generalized to branched chains in (Gregg and Spong, 2009b), with which we build directional 3-D walking gaits for a biped with a torso. In future work, this could potentially be applied to more complex bipeds with articulated arms that carry tools. We will then have to examine this method's

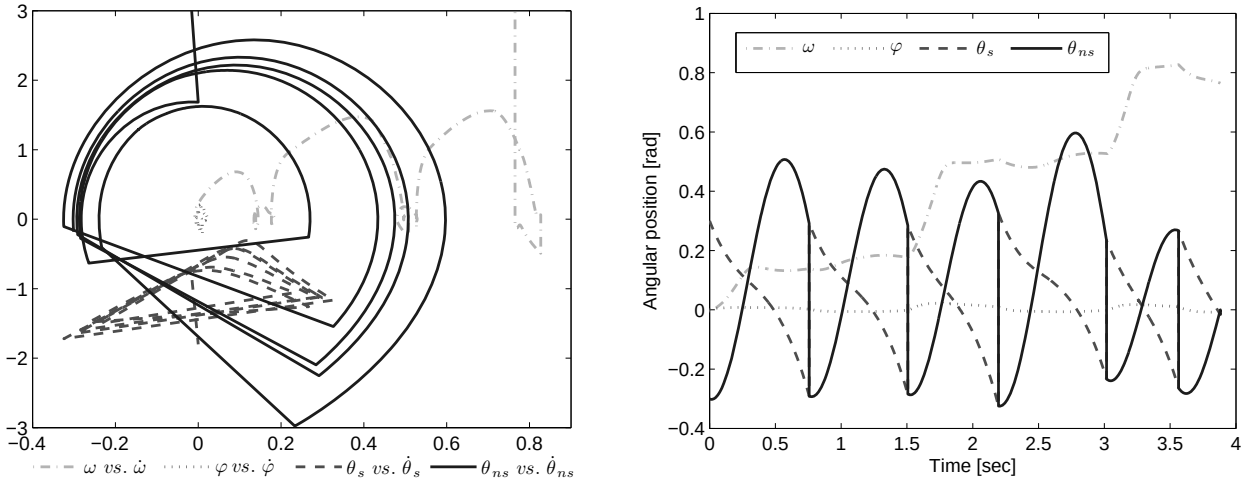

Fig. 8. Phase portrait (left) and trajectories (right) of failed turning maneuver using partial feedback linearization with small PD gains.

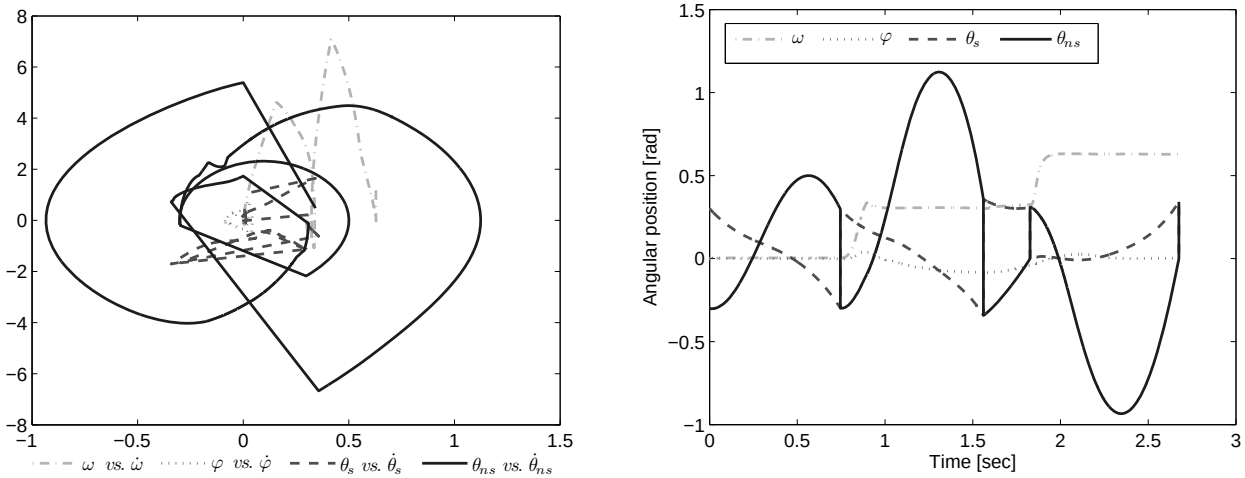

Fig. 9. Phase portrait (left) and trajectories (right) of failed turning maneuver using partial feedback linearization with large PD gains.

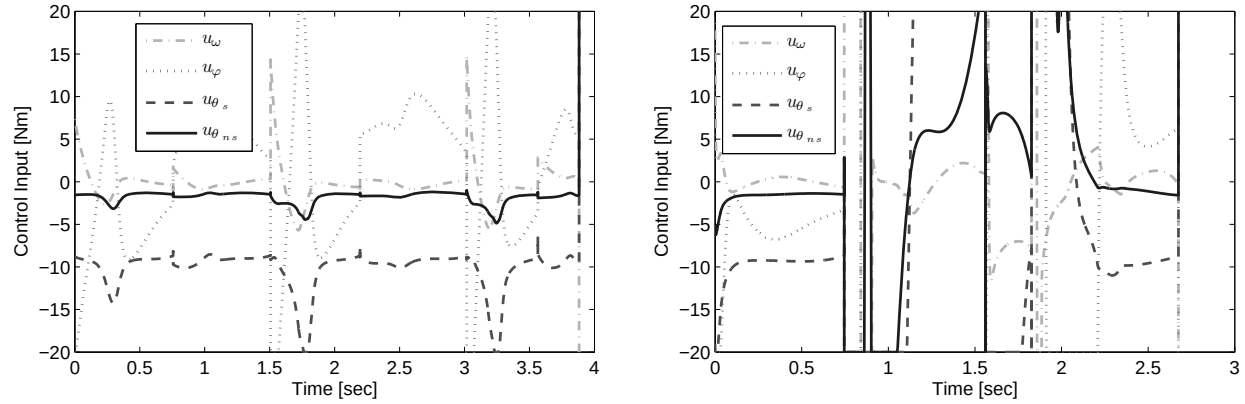

Fig. 10. Saturated control of the failed maneuvers using partial feedback linearization with small PD gains (left) and large PD gains (right).

robustness to model uncertainty. The underactuated case is still an open problem that demands further attention, but this should not pose a significant impediment to implementation if the biped's feet are designed to remain approximately flat during the entirety of each swing phase and impact event.

Reduction-based control theory is at the point of allowing passivity-based techniques to be effectively used in three dimensions. After addressing common implementation issues, complex robots with active control could embrace passive dynamics to walk dynamically towards desired locations to perform specific tasks. Such robots would have great autonomy from base stations, as the efficient and natural walking gaits would allow significant locomotion range and long battery life (arguably superior to related characteristics of quadrupedal and treaded robots (Kuo, 2007)). These are absolute necessities if robotic technologies are to be implemented on intelligent prosthetic legs or assisted walking devices for the elderly or disabled. There are similar applications in the manufacturing industry, where versatile and long-lasting robots are desirable for the varying demands of lean manufacturing environments. In general, our results are relevant as the medical, industrial, and military sectors become increasingly interested in legged robotics.

APPENDIX A
PROPERTIES OF ALMOST-CYCLIC LAGRANGIAN SYSTEMS

Since reduction-based control shapes the kinetic and potential characteristics of robots, we must consider whether the well-known properties of general robotic systems still hold. To begin, almost-cyclic systems do not preserve the linearity-in-the-parameters property, which provides that the E-L equations can be "linearly" expressed by

$$\frac{d}{dt}\frac{\partial L}{\partial \dot{q}} - \frac{\partial L}{\partial q} = Y(q, \dot{q}, \ddot{q})\Theta,$$

where $\Theta \in \mathbb{R}^p$ is the *parameter vector* of constants, in terms of link masses, inertias, and lengths, and $Y \in \mathbb{R}^{n \times p}$ is the *regressor* matrix of nonlinear functions of $(q, \dot{q}, \ddot{q})$, as discussed in (Spong et al., 2006). This property does not hold because reduction-based control laws require matrix inversion (demonstrated in Section V), introducing rational dependencies on q in the system dynamics and thus breaking linearity in the parameters. This can explicitly be seen in the almost-cyclic matrix $M_{\lambda_1^k}$ of (6).

On the other hand, several important properties of robotic systems do hold for k-ACL systems. After shaping a standard robot's Lagrangian to a k-ACL through a reduction-based control law like that of Section V, we prove the following properties are preserved:

1) Symmetry of the inertia matrix
2) Positive definiteness of the inertia matrix
3) Skew-symmetry of the inertia matrix minus twice the Coriolis matrix
4) Passivity of the system

A. Inertia Matrix

Theorem 3: Given a k-almost-cyclic Lagrangian, its inertia matrix $M_{\lambda_1^k}(q_2^n)$ is symmetric and positive definite.

Proof: Recall that k-almost-cyclic inertia matrix $M_{\lambda_1^k}(q_2^n)$ is defined in (6) by

$$M_{\lambda_1^k}(q_2^n) = M(q_2^n) + \sum_{i=1}^{k} \begin{pmatrix} 0_{i\times i} & 0_{i\times(n-i)} \\ 0_{(n-i)\times i} & \frac{M^T_{q_i,q^n_{i+1}}(q^n_{i+1})M_{q_i,q^n_{i+1}}(q^n_{i+1})}{m_{q_i}(q^n_{i+1})} \end{pmatrix}.$$

First, we know that inertia matrix $M(q_2^n)$ is symmetric and positive definite. Also, each summation term

$$\begin{pmatrix} 0_{i\times i} & 0_{i\times(n-i)} \\ 0_{(n-i)\times i} & \frac{M^T_{q_i,q^n_{i+1}}(q^n_{i+1})M_{q_i,q^n_{i+1}}(q^n_{i+1})}{m_{q_i}(q^n_{i+1})} \end{pmatrix}, \quad i \in \{1,k\},$$

is symmetric since the zero terms are trivially symmetric and since $m_{q_i}(q^n_{i+1})$ is scalar/symmetric and

$$\left(M^T_{q_i,q^n_{i+1}}(q^n_{i+1})M_{q_i,q^n_{i+1}}(q^n_{i+1})\right)^T = M^T_{q_i,q^n_{i+1}}(q^n_{i+1})M_{q_i,q^n_{i+1}}(q^n_{i+1}).$$

Each summation term is positive semidefinite since there are i zero-eigenvalues and since $m_{q_i}(q^n_{i+1})$ is positive definite by the positive definiteness of $M(q_2^n)$ and $M^T_{q_i,q^n_{i+1}}(q^n_{i+1})M_{q_i,q^n_{i+1}}(q^n_{i+1})$ is trivially positive definite. Finally, the sum of symmetric matrices is symmetric, and the sum of a positive definite matrix with positive semidefinite matrices is positive definite. ■

B. Skew-Symmetry

Given a k-almost-cyclic Lagrangian, its Coriolis-gyroscopic matrix is

$$C_{\lambda_1^k}(q,\dot{q}) = C_{M_{\lambda_1^k}}(q_2^n,\dot{q}) + C_{Q_{\lambda_1}}(q) + \ldots + C_{Q_{\lambda_k}}(q_k^n), \tag{29}$$

where $C_{M_{\lambda_1^k}}(q_2^n,\dot{q}) \in \mathbb{R}^{n\times n}$ is derived from $M_{\lambda_1^k}(q_2^n)$ and $C_{Q_{\lambda_i}}(q_i^n) \in \mathbb{R}^{n\times n}$ is derived from

$$Q_{\lambda_i}(q_i^n) = \begin{pmatrix} 0 & -\lambda_i(q_i)m_{q_i}^{-1}(q^n_{i+1})M_{q_i,q^n_{i+1}}(q^n_{i+1}) \end{pmatrix}^T, \quad i \in \{1,k\}.$$

Lemma 3: Matrix $C_{Q_{\lambda_i}}(q_i^n)$ is skew-symmetric $\forall i \in \{1,k\}$.

Proof: This is proven by calculation for any fixed $i \in \{1,k\}$:

$$C_{Q_{\lambda_i}}(q_i^n)\dot{q} = \frac{d}{dt}\nabla_{\dot{q}}[Q^T_{\lambda_i}(q_i^n)\dot{q}] - \nabla_q[Q^T_{\lambda_i}(q_i^n)\dot{q}],$$

where

$$\nabla_{\dot{q}}[Q^T_{\lambda_i}(q_i^n)\dot{q}] = \begin{pmatrix} 0_{i\times 1} \\ -\frac{\lambda_i(q_i)}{m_{q_i}(q^n_{i+1})}M^T_{q_i,q^n_{i+1}}(q^n_{i+1}) \end{pmatrix},$$

implying that

$$\frac{d}{dt}\nabla_{\dot{q}}[Q^T_{\lambda_i}(q_i^n)\dot{q}] = \begin{pmatrix} 0_{i\times 1} \\ -\frac{\dot{\lambda}_i(q_i)}{m_{q_i}(q^n_{i+1})}M^T_{q_i,q^n_{i+1}}(q^n_{i+1}) + \lambda_i(q_i)\frac{\dot{m}_{q_i}(q^n_{i+1})}{m^2_{q_i}(q^n_{i+1})}M^T_{q_i,q^n_{i+1}}(q^n_{i+1}) - \frac{\lambda_i(q_i)}{m_{q_i}(q^n_{i+1})}\dot{M}^T_{q_i,q^n_{i+1}}(q^n_{i+1}) \end{pmatrix}.$$

Also, the second term of $C_{Q_{\lambda_i}}(q_i^n)\dot{q}$ is given by

$$\nabla_q[Q_{\lambda_i}^T(q_i^n)\dot{q}] = \begin{pmatrix} 0_{(i-1)\times 1} \\ -\frac{\partial\lambda_i(q_i)}{\partial q_i}\frac{1}{m_{q_i}(q_{i+1}^n)}M_{q_i,q_{i+1}^n}(q_{i+1}^n)\dot{q}_{i+1}^n \\ -\frac{\lambda_i(q_i)}{m_{q_i}(q_{i+1}^n)}\frac{\partial M_{q_i,q_{i+1}^n}(q_{i+1}^n)}{\partial q_{i+1}^n}^T\dot{q}_{i+1}^n + \frac{\lambda_i(q_i)}{m_{q_i}^2(q_{i+1}^n)}M_{q_i,q_{i+1}^n}^T(q_{i+1}^n)\frac{\partial m_{q_i}(q_{i+1}^n)}{\partial q_{i+1}^n}^T\dot{q}_{i+1}^n \end{pmatrix}.$$

In this context, we have (note that $\frac{dy}{dt} := (\frac{\partial y}{\partial t})^T$ and $\frac{\partial(y^T)}{\partial x} = (\frac{\partial y}{\partial x})^T$ for all vectors x, y (Felippa, 2004)):

$$\begin{aligned} \dot{\lambda}_i(q_i) &= \frac{\partial\lambda_i(q_i)}{\partial q_i}\dot{q}_i \\ \dot{m}_{q_i}(q_{i+1}^n) &= \dot{m}_{q_i}^T(q_{i+1}^n) = \frac{\partial m_{q_i}(q_{i+1}^n)}{\partial q_{i+1}^n}^T\dot{q}_{i+1}^n \\ \dot{M}_{q_i,q_{i+1}^n}^T(q_{i+1}^n) &= \frac{\partial M_{q_i,q_{i+1}^n}(q_{i+1}^n)}{\partial q_{i+1}^n}^T\dot{q}_{i+1}^n, \end{aligned}$$

so after canceling terms we get

$$C_{Q_{\lambda_i}}(q_i^n)\dot{q} = \begin{pmatrix} 0_{(i-1)\times 1} \\ \frac{\partial\lambda_i(q_i)}{\partial q_i}\frac{1}{m_{q_i}(q_{i+1}^n)}M_{q_i,q_{i+1}^n}(q_{i+1}^n)\dot{q}_{i+1}^n \\ -\frac{\partial\lambda_i(q_i)}{\partial q_i}\frac{1}{m_{q_i}(q_{i+1}^n)}M_{q_i,q_{i+1}^n}^T(q_{i+1}^n)\dot{q}_i \end{pmatrix},$$

implying that

$$C_{Q_{\lambda_i}}(q_i^n) = \begin{pmatrix} 0_{(i-1)\times(i-1)} & 0_{(i-1)\times 1} & 0_{(i-1)\times(n-i)} \\ 0_{1\times(i-1)} & 0 & \frac{\partial\lambda_i(q_i)}{\partial q_i}\frac{1}{m_{q_i}(q_{i+1}^n)}M_{q_i,q_{i+1}^n}(q_{i+1}^n) \\ 0_{(n-i)\times(i-1)} & -\frac{\partial\lambda_i(q_i)}{\partial q_i}\frac{1}{m_{q_i}(q_{i+1}^n)}M_{q_i,q_{i+1}^n}^T(q_{i+1}^n) & 0_{(n-i)\times(n-i)} \end{pmatrix}.$$

Hence, $C_{Q_{\lambda_i}}$ is skew-symmetric. ■

Theorem 4: The skew-symmetry property holds for a k-almost-cyclic Lagrangian system, i.e., matrix $(\dot{M}_{\lambda_1^k} - 2C_{\lambda_1^k})$ is skew-symmetric.

Proof: According to Equation (29),

$$\dot{M}_{\lambda_1^k} - 2C_{\lambda_1^k} = (\dot{M}_{\lambda_1^k} - 2C_{M_{\lambda_1^k}}) - 2C_{Q_{\lambda_1}} - \ldots - 2C_{Q_{\lambda_k}}.$$

Since $M_{\lambda_1^k}$ is symmetric by Theorem 3, and $C_{M_{\lambda_1^k}}$ is derived from $M_{\lambda_1^k}$, it follows that $(\dot{M}_{\lambda_1^k} - 2C_{M_{\lambda_1^k}})$ is skew-symmetric (see the original skew-symmetry property in (Spong et al., 2006)). Moreover, the additional $C_{Q_{\lambda_i}}$ terms are skew-symmetric by Lemma 3. Finally, the summation of skew-symmetric terms is skew-symmetric. ■

C. Passivity

Due to the skew-symmetry property, the passivity property also holds for k-almost-cyclic robotic systems:

$$\dot{E}_\lambda = \dot{q}^T v \implies \int_0^t \dot{q}(\xi)^T v(\xi)d\xi \geq -\beta, \ \forall t > 0, \tag{30}$$

where v is the input for the k-almost-cyclic control system of (10) and $\beta \geq 0$.

Therefore, passivity-based control, such as the several forms described in (Spong, 2004) and (Spong et al., 2006), can be used on k-almost-cyclic robotic systems.

APPENDIX B
PROOF OF CONTROLLED REDUCTION THEOREM

We now prove Theorem 1 from Section II-D (note that this proof is based on the construction from (Ames, 2006)).

Proof: We begin this proof by inductively relating the v_{k+1}^n-controlled E-L equations of $L_{\lambda_1^k}$ to the k-reduced controlled E-L equations of L_{fct}. We will then be able to show the direct correspondence of solutions based on the uniqueness of solutions to well-behaved differential equations.

For the general case of reduction stage-j, where $j \in \{1, k-1\}$, we consider the generalized ACL[9] $L_{\lambda_j^k}$ in terms of its nested ACL and remaining term:

$$L_{\lambda_j^k}(q_j, q_{j+1}^n, \dot{q}_j, \dot{q}_{j+1}^n) = L_{\lambda_{j+1}^k}(q_{j+1}^n, \dot{q}_{j+1}^n) + \text{Rem}_j(q_j, q_{j+1}^n, \dot{q}_j, \dot{q}_{j+1}^n),$$

and similarly for the base case of stage-k, we have

$$L_{\lambda_k^k}(q_k, q_{k+1}^n, \dot{q}_k, \dot{q}_{k+1}^n) = L_{\text{fct}}(q_{k+1}^n, \dot{q}_{k+1}^n) + \text{Rem}_k(q_k, q_{k+1}^n, \dot{q}_k, \dot{q}_{k+1}^n),$$

where, for $l \in \{1, k\}$, the remaining term is apparent from (13b):

$$\begin{aligned}\text{Rem}_l(q_l^n, \dot{q}_l^n) &= \frac{1}{2} m_{q_l}(q_{l+1}^n)(\dot{q}_l)^2 + \dot{q}_l M_{q_l, q_{l+1}^n}(q_{l+1}^n)\dot{q}_{l+1}^n \\ &\quad + \frac{1}{2}\dot{q}_{l+1}^{n^T} \frac{M_{q_l, q_{l+1}^n}^T(q_{l+1}^n) M_{q_l, q_{l+1}^n}(q_{l+1}^n)}{m_{q_l}(q_{l+1}^n)} \dot{q}_{l+1}^n \\ &\quad - \frac{\lambda_l(q_l)}{m_{q_l}(q_{l+1}^n)} M_{q_l, q_{l+1}^n}(q_{l+1}^n)\dot{q}_{l+1}^n + \frac{1}{2}\frac{\lambda_l(q_l)^2}{m_{q_l}(q_{l+1}^n)}.\end{aligned}$$

Therefore, the controlled E-L equations for the general case are

$$\frac{d}{dt}\frac{\partial L_{\lambda_j^k}}{\partial \dot{q}_j} - \frac{\partial L_{\lambda_j^k}}{\partial q_j} = \frac{d}{dt}\frac{\partial \text{Rem}_j}{\partial \dot{q}_j} - \frac{\partial \text{Rem}_j}{\partial q_j} = 0 \tag{31}$$

$$\frac{d}{dt}\frac{\partial L_{\lambda_j^k}}{\partial \dot{q}_i} - \frac{\partial L_{\lambda_j^k}}{\partial q_i} = \frac{d}{dt}\frac{\partial L_{\lambda_{j+1}^k}}{\partial \dot{q}_i} - \frac{\partial L_{\lambda_{j+1}^k}}{\partial q_i} + \frac{d}{dt}\frac{\partial \text{Rem}_j}{\partial \dot{q}_i} - \frac{\partial \text{Rem}_j}{\partial q_i} = \begin{pmatrix} 0_{(k-j)\times 1} \\ B_{q_{k+1}^n} v_{k+1}^n \end{pmatrix} e_{i-j} \tag{32}$$

for $i \in \{j+1, n\}$, where e_{i-j} is the $(i-j)^{\text{th}}$ standard basis vector for $\mathbb{R}^{n-j}$. As for the base case, we have

$$\frac{d}{dt}\frac{\partial L_{\lambda_k^k}}{\partial \dot{q}_k} - \frac{\partial L_{\lambda_k^k}}{\partial q_k} = \frac{d}{dt}\frac{\partial \text{Rem}_k}{\partial \dot{q}_k} - \frac{\partial \text{Rem}_k}{\partial q_k} = 0 \tag{33}$$

$$\frac{d}{dt}\frac{\partial L_{\lambda_k^k}}{\partial \dot{q}_i} - \frac{\partial L_{\lambda_k^k}}{\partial q_i} = \frac{d}{dt}\frac{\partial L_{\text{fct}}}{\partial \dot{q}_i} - \frac{\partial L_{\text{fct}}}{\partial q_i} + \frac{d}{dt}\frac{\partial \text{Rem}_k}{\partial \dot{q}_i} - \frac{\partial \text{Rem}_k}{\partial q_i} = B_{q_{k+1}^n} v_{k+1}^n e_{i-k} \tag{34}$$

for $i \in \{k+1, n\}$, where e_{i-k} is the $(i-k)^{\text{th}}$ standard basis vector for $\mathbb{R}^{n-k}$.

It is now necessary to calculate the derivatives of $\text{Rem}_l(q_l^n, \dot{q}_l^n)$, for $l \in \{1, k\}$:

$$\frac{d}{dt}\frac{\partial \text{Rem}_l}{\partial \dot{q}_l} = \frac{d}{dt}(M_{q_l, q_{l+1}^n}(q_{l+1}^n))\dot{q}_{l+1}^n + M_{q_l, q_{l+1}^n}(q_{l+1}^n))\ddot{q}_{l+1}^n + m_{q_l}(q_{l+1}^n)\ddot{q}_l + \frac{d}{dt}(m_{q_l}(q_{l+1}^n))\dot{q}_l \tag{35}$$

$$\frac{\partial \text{Rem}_l}{\partial q_l} = -\frac{\frac{\partial}{\partial q_l}(\lambda_l(q_l))}{m_{q_l}(q_{l+1}^n)} M_{q_l, q_{l+1}^n}(q_{l+1}^n))\dot{q}_{l+1}^n + \frac{\lambda_l(q_l)\frac{\partial}{\partial q_1}(\lambda_l(q_l))}{m_{q_l}(q_{l+1}^n)} \tag{36}$$

[9]This generalized almost-cyclic Lagrangian is the parent of the j^{th} stage of reduction, as opposed to the target Routhian of the stage-j projection.

$$
\begin{aligned}
\frac{d}{dt}\frac{\partial \mathrm{Rem}_l}{\partial \dot{q}_i} &= \ddot{q}_{l+1}^{n\,T}\frac{M_{q_l,q_{l+1}^n}(q_{l+1}^n)^T M_{q_l,q_{l+1}^n}(q_{l+1}^n)}{m_{q_l}(q_{l+1}^n)}e_{i-1} + \dot{q}_{l+1}^{n\,T}\frac{\frac{d}{dt}(M_{q_l,q_{l+1}^n}(q_{l+1}^n))^T M_{q_l,q_{l+1}^n}(q_{l+1}^n)}{m_{q_l}(q_{l+1}^n)}e_{i-1} \\
&\quad + \dot{q}_{l+1}^{n\,T}\frac{M_{q_l,q_{l+1}^n}(q_{l+1}^n)^T \frac{d}{dt}(M_{q_l,q_{l+1}^n}(q_{l+1}^n))}{m_{q_l}(q_{l+1}^n)}e_{i-1} \\
&\quad - \frac{d}{dt}(m_{q_l}(q_{l+1}^n))\dot{q}_{l+1}^{n\,T}\frac{M_{q_l,q_{l+1}^n}(q_{l+1}^n)^T M_{q_l,q_{l+1}^n}(q_{l+1}^n)}{m_{q_l}(q_{l+1}^n)^2}e_{i-1} \\
&\quad + \ddot{q}_l M_{q_l,q_{l+1}^n}(q_{l+1}^n)e_{i-1} + \dot{q}_l\frac{d}{dt}(M_{q_l,q_{l+1}^n}(q_{l+1}^n))e_{i-1} \\
&\quad + \frac{\lambda_l(q_l)\frac{d}{dt}(m_{q_l}(q_{l+1}^n))}{m_{q_l}(q_{l+1}^n)^2}M_{q_l,q_{l+1}^n}(q_{l+1}^n)e_{i-1} \\
&\quad - \frac{\frac{d}{dt}(\lambda_l(q_l))}{m_{q_l}(q_{l+1}^n)}M_{q_l,q_{l+1}^n}(q_{l+1}^n)e_{i-1} - \frac{\lambda_l(q_l)}{m_{q_l}(q_{l+1}^n)}\frac{d}{dt}(M_{q_l,q_{l+1}^n}(q_{l+1}^n))e_{i-1} \qquad (37)
\end{aligned}
$$

$$
\begin{aligned}
\frac{\partial \mathrm{Rem}_l}{\partial q_i} &= 2\dot{q}_{l+1}^{n\,T}\frac{\frac{\partial}{\partial q_i}(M_{q_l,q_{l+1}^n}(q_{l+1}^n))^T M_{q_l,q_{l+1}^n}(q_{l+1}^n)}{2m_{q_l}(q_{l+1}^n)}\dot{q}_{l+1}^n \\
&\quad - \dot{q}_{l+1}^{n\,T}\frac{\frac{\partial}{\partial q_i}(m_{q_l}(q_{l+1}^n))M_{q_l,q_{l+1}^n}(q_{l+1}^n)^T M_{q_l,q_{l+1}^n}(q_{l+1}^n)}{2m_{q_l}(q_{l+1}^n)^2}\dot{q}_{l+1}^n \\
&\quad + \frac{1}{2}\frac{\partial}{\partial q_i}(m_{q_l}(q_{l+1}^n))(\dot{q}_{l+1})^2 + \dot{q}_l\frac{\partial}{\partial q_i}(M_{q_l,q_{l+1}^n}(q_{l+1}^n))\dot{q}_{l+1}^n \\
&\quad + \frac{\frac{\partial}{\partial q_i}(m_{q_l}(q_{l+1}^n))\lambda_l(q_l)}{m_{q_l}(q_{l+1}^n)^2}M_{q_l,q_{l+1}^n}(q_{l+1}^n)\dot{q}_{l+1}^n \\
&\quad - \frac{\lambda_l(q_l)}{m_{q_l}(q_{l+1}^n)}\frac{\partial}{\partial q_i}(M_{q_l,q_{l+1}^n}(q_{l+1}^n))\dot{q}_{l+1}^n - \frac{1}{2}\frac{\frac{\partial}{\partial q_i}(m_{q_l}(q_{l+1}^n))\lambda_l(q_l)^2}{m_{q_l}(q_{l+1}^n)^2}, \qquad (38)
\end{aligned}
$$

where $i \in \{l+1, n\}$. Given these expressions, we can prove that the E-L equations for Rem_l hold given constraint (18). In particular, (18) implies the following derivative of $\lambda_l(q_l)$ and second derivative of q_l:

$$
\begin{aligned}
\frac{d}{dt}(\lambda_l(q_l)) &= \frac{\partial}{\partial q_l}(\lambda_l(q_l))\dot{q}_l = \frac{\partial \mathrm{Rem}_l}{\partial q_l}, \qquad (39) \\
\ddot{q}_l &= \frac{\frac{d}{dt}(m_{q_l}(q_{l+1}^n))}{m_{q_l}(q_{l+1}^n)^2}M_{q_l,q_{l+1}^n}(q_{l+1}^n)\dot{q}_{l+1}^n - \frac{\frac{d}{dt}(m_{q_l}(q_{l+1}^n))}{m_{q_l}(q_{l+1}^n)^2}\lambda_l(q_l) \qquad (40) \\
&\quad + \frac{\frac{d}{dt}(\lambda_l(q_l))}{m_{q_l}(q_{l+1}^n)} - \frac{\frac{d}{dt}(M_{q_l,q_{l+1}^n}(q_{l+1}^n))}{m_{q_l}(q_{l+1}^n)}\dot{q}_{l+1}^n - \frac{M_{q_l,q_{l+1}^n}(q_{l+1}^n)}{m_{q_l}(q_{l+1}^n)}\ddot{q}_{l+1}^n.
\end{aligned}
$$

Then, (35) & (36) given (18), (39), (40) $\Longrightarrow$

$$
\left[\frac{d}{dt}\frac{\partial \mathrm{Rem}_l}{\partial \dot{q}_l} - \frac{\partial \mathrm{Rem}_l}{\partial q_l}\right]\Bigg|_{J_l(q_l^n,\dot{q}_l^n)=\lambda_l(q_l)} = 0. \qquad (41)
$$

And, (37) given (18) & (40) $\Longrightarrow$

$$
\frac{d}{dt}\frac{\partial \mathrm{Rem}_l}{\partial \dot{q}_i}\Bigg|_{J_l(q_l^n,\dot{q}_l^n)=\lambda_l(q_l)} = 0.
$$

And, (38) given (18) $\Longrightarrow$

$$
\frac{\partial \mathrm{Rem}_l}{\partial q_i}\Bigg|_{J_l(q_l^n,\dot{q}_l^n)=\lambda_l(q_l)} = 0.
$$

Hence, we have

$$
\left[\frac{d}{dt}\frac{\partial \mathrm{Rem}_l}{\partial \dot{q}_i} - \frac{\partial \mathrm{Rem}_l}{\partial q_i}\right]\Bigg|_{J_l(q_l^n,\dot{q}_l^n)=\lambda_l(q_l)} = 0, \qquad (42)
$$

for $i = l+1, \ldots, n$, showing that the E-L equations for Rem_l hold given that the functional quantities are conserved.

Then, by the single-stage reduction proof of (Ames et al., 2007), based on the uniqueness of solutions to well-behaved differential equations, we know that solutions can be related through the single-stage reduction of both the general case and the base case. Hence, the multistage theorem follows by induction, proving the relationship between solutions of full-order vector field $\hat{f}_{\lambda_1^k}$ and solutions of k-reduced vector field $\hat{f}_{\mathrm{fct}}$. ■

APPENDIX C
FOUR-DOF BIPED INERTIA MATRIX TERMS

The inertia matrix for the 4-DOF biped defined in Section IV has the form

$$\begin{aligned} M_{4\mathrm{D}}(\varphi,\theta) &= \begin{pmatrix} m_\omega(\varphi,\theta) & M_{\omega,\varphi,\theta}(\varphi,\theta) \\ M^T_{\omega,\varphi,\theta}(\varphi,\theta) & M_{3\mathrm{D}}(\theta) \end{pmatrix} \\ &= \begin{pmatrix} m_\omega(\varphi,\theta) & \multicolumn{2}{c}{\multirow{2}{*}{—}} \\ | & & \\ M^T_{\omega,\varphi,\theta}(\varphi,\theta) & m_\varphi(\theta) & M_{\varphi,\theta}(\theta) \\ & M^T_{\varphi,\theta}(\theta) & M_\theta(\theta) \end{pmatrix}. \end{aligned}$$

Here, the sagittal 2-D-subsystem's inertia matrix is

$$M_\theta(\theta) = \begin{pmatrix} \frac{l^2}{4}(5m+4M)\cos(\rho)^2 & -\frac{l^2 m}{2}\cos(\theta_s-\theta_{ns})\cos(\rho)^2 \\ -\frac{l^2 m}{2}\cos(\theta_s-\theta_{ns})\cos(\rho)^2 & \frac{l^2 m}{4}\cos(\rho)^2 \end{pmatrix},$$

and the remaining terms for inertia submatrix $M_{3\mathrm{D}}$ are given by

$$\begin{aligned} m_\varphi(\theta) &= \frac{1}{32}(4l^2(13m+6M)+8(4m+M)w^2 \\ &\quad +l(-4l(7m+2M)\cos(2\rho)+lm\cos(2(\rho-\theta_{ns}))+2lm\cos(2\theta_{ns}) \\ &\quad +lm\cos(2(\rho+\theta_{ns}))+4(l\cos(\rho)^2(-8m\cos(\theta_{ns})\cos(\theta_s)+(5m+4M)\cos(2\theta_s)) \\ &\quad -8(3m+M)w\sin(\rho)))) \\ M_{\varphi,\theta}(\theta) &= \begin{pmatrix} -\frac{l}{4}\cos(\rho)(-2(2m+M)w+l(7m+4M)\sin(\rho))\sin(\theta_s) \\ \frac{lm}{4}\cos(\rho)(-2w+3l\sin(\rho))\sin(\theta_{ns}) \end{pmatrix}^T. \end{aligned}$$

Finally, the remaining matrix terms in $M_{4\mathrm{D}}$ are

$$
\begin{aligned}
m_\omega(\varphi,\theta) &= \frac{1}{16}(2l(4l\cos(\rho)^2(3m+2M-2m\cos(\theta_{ns}-\theta_s))\sin(\varphi)^2 \\
&\quad +4w\cos(\rho)(-m\cos(\theta_{ns})+(2m+M)\cos(\theta_s))\sin(2\varphi) \\
&\quad -l(-3m\cos(\theta_{ns})+(7m+4M)\cos(\theta_s))\sin(2\rho)\sin(2\varphi)) \\
&\quad -\cos(\varphi)^2(-2(l^2(13m+6M)+2(4m+M)w^2) \\
&\quad +l^2\cos(2\rho)(14m+4M+m\cos(2\theta_{ns})+(5m+4M)\cos(2\theta_s)+8m\sin(\theta_{ns})\sin(\theta_s)) \\
&\quad +l(lm\cos(2\theta_{ns})+l(5m+4M)\cos(2\theta_s) \\
&\quad +8(2(3m+M)w\sin(\rho)+lm\sin(\theta_{ns})\sin(\theta_s)))))
\end{aligned}
$$

$$
M_{\omega,\varphi,\theta}(\varphi,\theta) = \begin{pmatrix} m_{\omega,\varphi}(\varphi,\theta) & m_{\omega,\theta_s}(\varphi,\theta) & m_{\omega,\theta_{ns}}(\varphi,\theta) \end{pmatrix}
$$

$$
\begin{aligned}
m_{\omega,\varphi}(\varphi,\theta) &= \frac{1}{8}l(4w\cos(\rho)\sin(\varphi)(-m\sin(\theta_{ns})+(2m+M)\sin(\theta_s)) \\
&\quad -l\sin(2\rho)\sin(\varphi)(-3m\sin(\theta_{ns})+(7m+4M)\sin(\theta_s)) \\
&\quad -l\cos(\rho)^2\cos(\varphi)(m\sin(2\theta_{ns})+(5m+4M)\sin(2\theta_s)-4m\sin(\theta_{ns}+\theta_s)))
\end{aligned}
$$

$$
\begin{aligned}
m_{\omega,\theta_s}(\varphi,\theta) &= \frac{1}{8}l(4(2m+M)w\cos(\rho)\cos(\varphi)\cos(\theta_s)-l(7m+4M)\cos(\varphi)\cos(\theta_s)\sin(2\rho) \\
&\quad +2l\cos(\rho)^2(5m+4M-2m\cos(\theta_{ns}-\theta_s))\sin(\varphi))
\end{aligned}
$$

$$
m_{\omega,\theta_{ns}}(\varphi,\theta) = -\frac{1}{4}lm\cos(\rho)(\cos(\varphi)\cos(\theta_{ns})(2w-3l\sin(\rho))+l\cos(\rho)(-1+2\cos(\theta_{ns}-\theta_s))\sin(\varphi)).
$$

ACKNOWLEDGMENTS

The authors would like to thank Aaron D. Ames for pioneering the ideas that led to this project, Prashant G. Mehta for offering an important perspective on symmetry and symmetry-breaking, and Eric D.B. Wendel for coding the original version of the simulation package. We also thank NSF Grant CMS-0510119 for supporting this project.

REFERENCES

Ames, A. D. 2006. A Categorical Theory of Hybrid Systems. PhD thesis, University of California, Berkeley.

Ames, A. D. and Gregg, R. D. 2007. Stably extending two-dimensional bipedal walking to three dimensions. In: American Control Conference, New York, NY.

Ames, A. D., Gregg, R. D., and Spong, M. W. 2007. A geometric approach to three-dimensional hipped bipedal robotic walking. In: Conference on Decision and Control, New Orleans, LA.

Ames, A. D., Gregg, R. D., Wendel, E. D. B., and Sastry, S. 2006. Towards the geometric reduction of controlled three-dimensional robotic bipedal walkers. In: 3rd Workshop on Lagrangian and Hamiltonian Methods for Nonlinear Control (LHMNLC'06), Nagoya, Japan.

Byl, K. and Tedrake, R. 2008. Metastable walking on stochastically rough terrain. In: Robotics: Science and Systems IV.

Chevallereau, C., Abba, G., Aoustin, Y., Plestan, F., Westervelt, E. R., Canudas-de-Wit, C., and Grizzle, J. W. 2003. Rabbit: A testbed for advanced control theory. IEEE Control Systems Magazine, 23(5):57–79.

Chevallereau, C., Grizzle, J. W., and Shih, C. 2008. Asymptotically stable walking of a five-link underactuated 3D bipedal robot. IEEE Transactions on Robotics, 25(1):37–50.

Collins, S. H., Wisse, M., and Ruina, A. 2001. A 3-D passive dynamic walking robot with two legs and knees. International Journal of Robotics Research, 20:607–615.

Felippa, C. A. 2004. Appendix D: Matrix calculus. In: Introduction to Finite Element Methods, Boulder. University of Colorado at Boulder.

Fukuda, T., Doi, M., Hasegawa, Y., and Kajima, H. 2006. Fast Motions in Biomechanics and Robotics, chapter Multi-Locomotion Control of Biped Locomotion and Brachiation Robot, pages 121–145. Lecture Notes in Control and Information Sciences. Springer, Heidelberg, Allemagne.

Goswami, A., Thuilot, B., and Espiau, B. 1996. Compass-like biped robot part I: Stability and bifurcation of passive gaits. Technical Report 2996, Institut National de Recherche en Informatique et en Automatique.

Gregg, R. D. and Spong, M. W. 2008. Reduction-based control with application to three-dimensional bipedal walking robots. In: American Control Conference, Seattle, WA.

Gregg, R. D. and Spong, M. W. 2009a. Bringing the compass-gait bipedal walker to three dimensions. In: IEEE International Conference on Intelligent Robots and Systems, St. Louis, MO.

Gregg, R. D. and Spong, M. W. 2009b. Reduction-based control of branched chains: Application to three-dimensional bipedal torso robots. In: Conference on Decision and Control, Shanghai, China.

Grizzle, J. W., Abba, G., and Plestan, F. 2001. Asymptotically stable walking for biped robots: Analysis via systems with impulse effects. IEEE Transactions on Automatic Control, 46(1):51–64.

Krstic, M., Kanellakopoulos, I., and Kokotovic, P. V. 1995. Nonlinear and Adaptive Control Design. Wiley, Inc., New York, New York.

Kuo, A. D. 1999. Stabilization of lateral motion in passive dynamic walking. International Journal of Robotics Research, 18(9):917–930.

Kuo, A. D. 2007. Choosing your steps carefully: Walking and running robots. IEEE Robotics and Automation Magazine, 14(2):18–29.

Leonard, N. E. 1997. Stabilization of underwater vehicle dynamics with symmetry-breaking potentials. Systems and Control Letters, 32:35–42.

Marsden, J. E. and Ratiu, T. S. 2002. Introduction to Mechanics and Symmetry. Springer, New York, NY, 2 edition.

McGeer, T. 1990. Passive dynamic walking. International Journal of Robotics Research, 9(2):62–82.

Mehta, P. G., Hagen, G., and Banaszuk, A. 2007. Symmetry and symmetry-breaking for a wave equation with feedback. SIAM Journal of Applied Dynamical Systems.

Morris, B. and Grizzle, J. W. 2006. A restricted Poincaré map for determining exponentially stable periodic orbits in systems with impulse effects: Application to bipedal robots. In: Conference on Decision and Control, Seville, Spain.

Murray, R. M., Li, Z., and Sastry, S. S. 1994. A Mathematical Introduction to Robotic Manipulation. CRC Press.

Sastry, S. S. 1999. Nonlinear Systems: Analysis, Stability and Control. Springer-Verlag, New York, NY.

Shammas, E. A., Choset, H., and Rizzi, A. A. 2007a. Geometric motion planning analysis for two classes of underactuated mechanical systems. International Journal of Robotics Research, 26(10):1043–1073.

Shammas, E. A., Choset, H., and Rizzi, A. A. 2007b. Towards a unified approach to motion planning for dynamic underactuated mechanical systems with non-holonomic constraints. International Journal of Robotics Research, 26(10):1075–1124.

Spong, M. W. 1999. Passivity based control of the compass gait biped. In: IFAC World Congress, Beijing, China.

Spong, M. W. 2004. The passivity paradigm in bipedal locomotion. In: International Conference on Climbing and Walking Robots, Madrid, Spain.

Spong, M. W. and Bullo, F. 2002. Controlled symmetries and passive walking. In: IFAC World Congress, Barcelona, Spain.

Spong, M. W. and Bullo, F. 2005. Controlled symmetries and passive walking. IEEE Transactions on Automatic Control, 50(7):1025–1031.

Spong, M. W., Holm, J. K., and Lee, D. 2007. Passivity-based control of bipedal locomotion. IEEE Robotics Automation Magazine, 12(2):30–40.

Spong, M. W., Hutchinson, S., and Vidyasagar, M. 2006. Robot Modeling and Control. John Wiley and Sons, Inc., Hoboken, NJ.

Tedrake, R., Zhang, T. W., and Seung, H. S. 2004. Stochastic policy gradient reinforcement learning on a simple 3d biped. In: IEEE International Conference on Intelligent Robots and Systems, Sendai, Japan.

Westervelt, E. R., Grizzle, J. W., and Koditschek, D. E. 2003. Hybrid zero dynamics of planar biped walkers. IEEE Transactions on Automatic Control, 48(1).